Investigation of Ultimate Strength of Composite Open-Web Joist-Girders

Sheldon L. Showalter

Thesis submitted to the Faculty of the
Virginia Polytechnic Institute and State University
in partial fulfillment of the requirements for the degree of

Master of Science
in
Civil Engineering

W. Samuel Easterling, Chair
Thomas M. Murray
Richard M. Barker

September 16, 1999
Blacksburg, Virginia

Keywords: Composite Joist-Girder, Flush Framed Joist-Girder, Stub-Girder, Haunched Girder

Investigation of Ultimate Strength of Composite Open-Web Joist-Girders

Sheldon L. Showalter

ABSTRACT

The goal of this research was to study several methods of generating composite action using open-web joist-girders, designed and manufactured by Nucor Corporation. In addition to comparing the relative performance of these systems, it was intended to determine whether the current accepted design procedure for composite joists could be extended to joist-girders.

ACKNOWLEDGMENTS

I would like to thank everyone who has had a part in the preparation of this thesis. First of all, I would like to thank my Lord and Savior, Jesus Christ, without whom nothing in this life would have meaning. I would also like to give special thanks to my wife, Jenny, who has been very patient with me and has been a tremendous encouragement to me during the writing process. Thank you to my parents for giving me the opportunity to attend Virginia Tech, and to my extended family for all of the moral support. I would like to thank Dr. W. S. Easterling for serving as my advisor and committee chairman. Thanks also to Dr. T. M. Murray and Dr. R. M. Barker for offering your expertise to shape the final report of this work.

I would like to thank Nucor Corporation for the opportunity to perform this testing. I would especially like to thank David Samuelson, of Nucor Research and Development, for designing the tests and for answering many questions along the way. I thank Brett Farmer and Dennis Huffman for their many hours of assistance with the construction and testing of these floor systems. I would also like to thank my fellow graduate students who had their hands in the process a little or a lot, Michelle Rambo-Roddenberry, Budi Wujija, Ric Anderson, Cindy Kraus, James Young and Joe Howard.

TABLE OF CONTENTS

Page

LIST OF FIGURES

LIST OF TABLES

LIST OF SYMBOLS

a	Effective concrete flange thickness, in.
A_{BC}	Cross-sectional area of bottom chord, in.^{2}
A_s	Cross-sectional area of steel in tension, in.^{2}
A_{TC}	Cross-sectional area of top chord, in.^{2}
b_1	Effective width of concrete slab, in.
C_{slip}	Shear stud slip coefficient
d_{eBC}	Distance from the line of action of the compressive force in the concrete slab to the centroid of bottom chord, in.
d_{eTC}	Distance from the line of action of the compressive force in the concrete slab to the centroid of top chord, in.
E_c	Modulus of elasticity of concrete, ksi
E_s	Modulus of elasticity of steel, ksi
f_c'	Compressive strength of concrete, ksi
F_y	Tensile yield stress, ksi or psi
F_{yBC}	Measured yield stress of bottom chord, ksi or psi
F_{yTC}	Measured yield stress of top chord, ksi or psi
F_u	Tensile ultimate stress, ksi or psi
H	Total depth of slab and joist-girder, in.
h	Depth of concrete slab, in.
I	Moment of inertia, in.^{4}
I_{exp}	Experimental moment of inertia, in.^{4}
I_{calc}	Predicted moment of inertia, in.^{4}
I_{exp}	Experimental moment of inertia, in.^{4}
I_{nc}	Non-composite moment of inertia, in.^{4}
I_t	Transformed moment of inertia, in.^{4}
M	Midspan moment due to total load, ft-kips
M_{dm}	Predicted midspan design moment based on measured material properties, ft-kips
M_{dn}	Predicted midspan design moment based on nominal material properties, ft-kips
M_{ym}	Predicted midspan yield moment based on measured material properties, ft-kips
M_{yn}	Predicted midspan yield moment based on nominal material properties, ft-kips

n	Modular ratio, E_s/E_c
P	Concentrated applied load, kips
ΣQ	Shear connector capacity, kips
R_L	Concentrated load, kips
R_{sj}	Concentrated dead load due to self-weight of slab and joist, kips
T	Bottom chord tension force due to total load, kips
TL	Total load due to combined dead and applied loads, kips
TL_{dm}	Predicted total design load based on measured material properties, kips
TL_{dn}	Predicted total design load based on nominal material properties, kips
TL_e	Experimental total load, kips
TL_{ym}	Predicted total yield load based on measured material properties, kips
TL_{yn}	Predicted total yield load based on nominal material properties, kips
WEF	"Web Effects Factor" – the ratio of theoretical deflection in an open-web joist to the deflection based on a static analysis
w_g	Unit weight of concrete, pcf
w_g	Uniformly distributed joist-girder self-weight, klf
x	Distance of applied load from girder end, ft
Δ_{adj}	Span / Depth adjustment factor developed by Nucor
Δ_{calc}	Predicted deflection at design load based on measured material properties, in.
Δ_{exp}	Experimental deflection at design load, in.
Δ_{Vmax}	Maximum deflection of total load case found using a stiffness analysis program developed by Nucor which accounts for web shortening, in.
Δ_{wwe}	Deflection (without web effects) based on a static beam analysis including dead and applied loads, in.

CHAPTER I
INTRODUCTION

1.1 Background

As the use of long-span composite open-web joists has increased, there has been a corresponding growth of interest in developing better and more efficient applications of this type of structural system. Historically, composite design has been applied only to joists that directly support a concrete deck slab. That is, the steel deck spans perpendicular to these joists and rests directly on their top chords. The girders supporting these joists are traditionally hot-rolled open-web joist-girders or wide flange beams that are not composite because they do not come in direct contact with the deck and slab. A gap is left between the deck and girder top chords or flanges because of the joist bearing seats, as shown in Figure 1.1.

As a result of this limitation, composite joist testing has focused on joists that directly support the deck sheeting and concrete slab. Based on the literature available on this testing, a specification (*Proposed* 1996) was prepared to supplement the Load and Resistance Factor Design (LRFD) Specification for Structural Steel Buildings of the American Institute of Steel Construction (AISC 1993). This specification provides a model for designing composite joists where the controlling limit state is yielding of the bottom chord members.

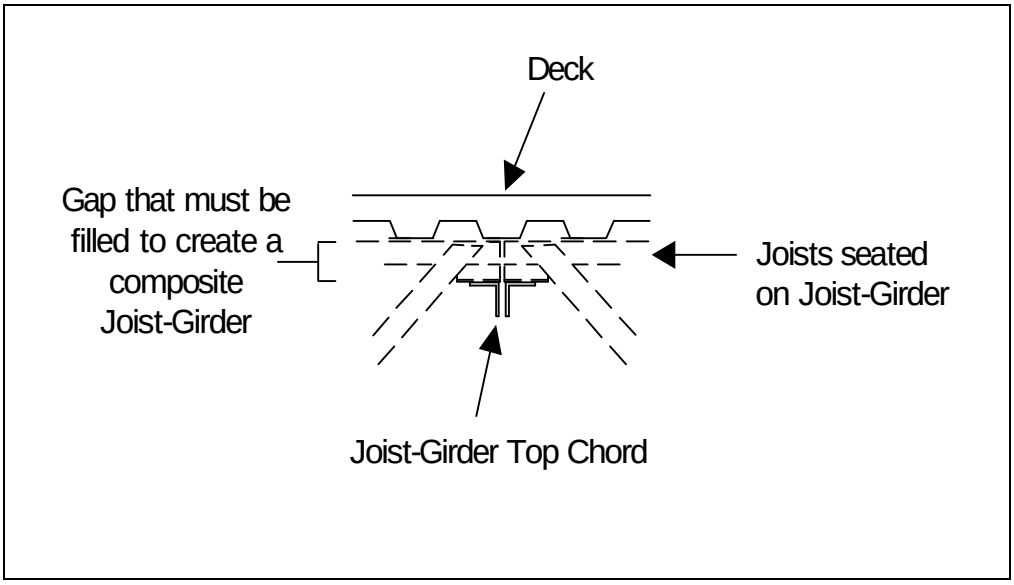

Figure 1.1 Depiction of Gap Between Slab and Joist-Girder

With the increased use of composite joists, and the success of composite design, it is of interest to know how well joist-girders may respond when designed as composite members. Nucor Research and Development sponsored this research to look at several specific issues. First, the primary consideration in creating a floor system with composite joist-girders is deciding how to frame the joists into the joist-girders so that the deck is brought into contact with the girder top chords such that shear connectors may be attached to those top chords. Secondly, testing of joist-girders that act as part of a full structural system where the girders receive concentrated loads from joists has not been reported.

Three distinct configurations were considered to develop composite action in an open-web steel joist-girder. A flush framed specimen was developed where the gap was eliminated by the use of special bolted connections. This allowed all of the top chords to be positioned at the same elevation, as shown in Figure 1.2.

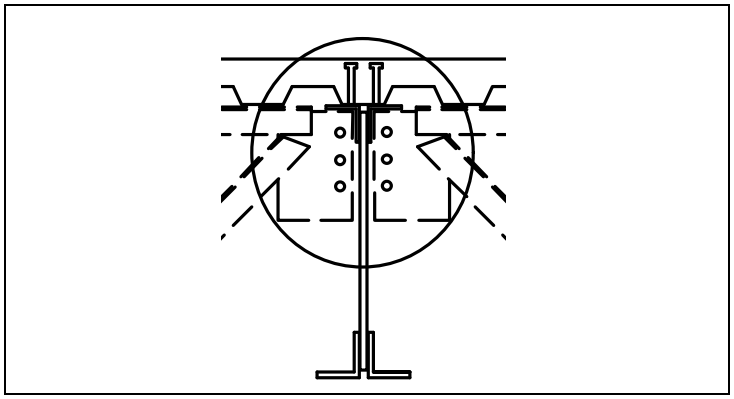

Figure 1.2 Flush Framed Girder Connection Detail

A stub girder specimen was developed to fill the gap by attaching small H-shapes or “stubs” to the joist-girder top chords, as shown in Figure 1.3.

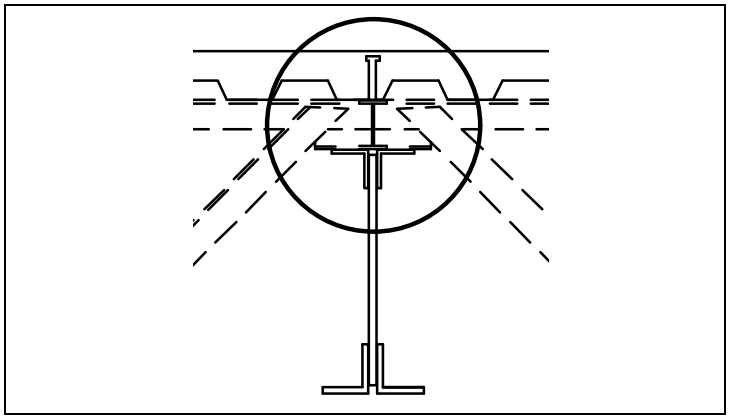

Figure 1.3 Stub-Girder Connection Detail

Finally, a haunched girder specimen was developed to fill the gap by forming haunches over the joist-girders to bring the slab into contact with the top chords, as shown in Figure 1.4.

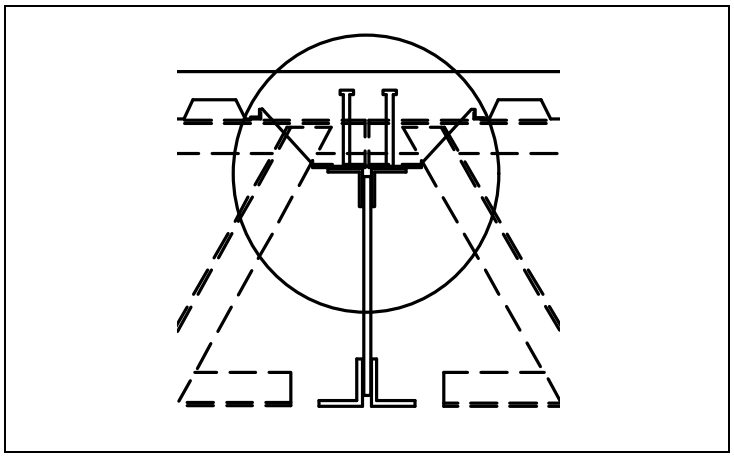

Figure 1.4 Haunched Girder Connection Detail

The details of these specimens and the results of testing are discussed in the following chapters.

1.2 Literature Review

Research on composite joist systems has grown significantly over the last 30 years. The resulting literature laid the foundation for the development of design and analysis methodologies for this structural system. Each specimen being investigated employed a distinct configuration to achieve composite action, so it was important to explore the background of each. First, material published regarding general composite design using open-web steel joists is reviewed. Then, research on stub girders is considered. Literature discussing the design of concrete haunches, formed in conjunction with composite girders, is also examined.

1.2.1 Composite Joist Research

Laboratory testing and development of design procedures for composite open-web steel joists has been underway for several decades. Early research by Tide and Galambos (1968) looked at the interaction of a joist and slab with emphasis on how shear connectors would perform and what the capacities of those connectors would be. The authors noted that the tension chord yield strength and the distance of the tension chord from the compression chord were the principal factors in determining the theoretical capacity of a composite joist. Also, the degree of composite action was found to be dependent more on

the stiffness of the shear connectors than on the type of connector used. The authors also noted that for heavy slabs, where the slab thickness was substantial with respect to the chord depth, the slab stress was much less than the bottom chord stress, even at the point where the bottom chord was yielding.

Further research was conducted and reported on a few years later by Azmi (1972). Six composite joist configurations were investigated. Azmi's objective was to develop a design methodology for composite open-web joists with metal decking. The specimens were all composed of single joists supporting 5 ft wide slabs and spanning 50 ft. The slabs were constructed with 2.5 in. of cover on 1.5 in. deep steel decking and utilized 3 in. high, 0.5 in. diameter shear studs. In his analysis, Azmi derived an ultimate strength method for the design of composite joists that agreed well with experimental results. In general, he found that the measured bottom chord strains and deflections were larger than those predicted by elastic analytical approaches.

The joists designed to achieve full connection capacity were observed to fail by fracture of the bottom chord or by buckling of a web member. The joists designed to achieve only partial connection failed by buckling of the top chord. From his observations, Azmi established a classification system for joists having three distinct categories. The joists were classified as over-connected, balanced, or under-connected, depending upon the amount of connection achieved. The categories were defined by whether the ultimate strengths of the shear connectors were greater than, equal to, or less than the maximum tensile forces that could be developed in the bottom chords. An elastic method for calculating stresses, based on the assumption that the concrete area in compression acts as an equivalent area of steel, was used to analyze all specimens.

Fahmy (1974) introduced the use of a finite difference method to calculate strains, stresses, deflections and the interacting forces in a system for both elastic and inelastic behavior. Inelastic behavior was an issue if the load-slip relationship for the shear connectors was non-linear or if the stress-strain relationship for either the steel joist or the concrete slab was non-linear.

Chien and Ritchie (1984) were responsible for one of the most comprehensive early texts devoted to composite design. An entire chapter covered the design of composite open-web steel joists and trusses. The authors presented comprehensive design criteria that had previously appeared in the Canadian Code CAN3-S16.1-M84, commonly referred to as S16.1. These criteria were for an ultimate strength design that focused on the force equilibrium of the composite cross-section. The authors also provided guidelines for a manual calculation process as well as a brief proposal for modeling a composite system with a computerized stiffness analysis.

Curry (1988) reported on two full-scale tests of long-span composite joists. He presented a detailed computer analysis of the systems that made use of a second order, linear finite element analysis. He proposed four slightly different models of the composite system for comparison. The models varied in how they accounted for the shear connectors. The models were evaluated by comparing the data calculated for the

predicted yield loads and the predicted maximum loads with the data found experimentally. Test results agreed with previous research that showed that beam theory could predict strains in the bottom chord, assuming that web buckling, top chord buckling and shear stud failure were all prevented.

The best approximation of the experimental results was found according to the model that used an AISC LRFD lower bound moment of inertia estimate of the top chord area. The model also viewed the shear studs as small beams fixed at the connection to the top chord and pinned at the concrete deck connection. This model predicted member forces better than the other methods used. It was found, however, that the model significantly over-predicted the deflections of the joists. The best prediction of deflections was achieved through a combination of methods that had been previously proposed by researchers. The author also used the idea of a "load index" to compare different designs. This index is simply the ratio of the ultimate design capacity to the actual load at yield, and can be applied to any of the various specimen components. These component indexes could then be used to identify structure proportions that would result in particular failure modes.

Gibbings et al (1991) reported on eight full-scale, single span, composite open-web joists. Analytical methods were presented and a non-linear finite element model was formulated. Non-linear behavior was obtained in the model by using plastic beam elements to represent the bottom chord. The model also included linear elastic beam elements representing the top chord and shear studs. The studs were modeled as very small elastic beams with nearly infinite stiffnesses. The concrete and web members were modeled with truss elements, using nominal cross-sectional areas and moments of inertia. The bottom chords were modeled using actual measured yield stress values.

Nguyen (1992) worked to develop a finite element model for long-span composite joists having incomplete interaction. Seven test specimens, several of which had been previously reported (Gibbings et al 1991), were used to test and improve the accuracy of the model. The flexibility of the shear connectors and the behavior of the elastic-plastic material were considered. The model behaved reasonably well in comparison with the specimens. While being easy to generate, and although it predicted deflections well, the model gave fairly unconservative values for the ultimate load capacity. The model tended to give better deflection results than the method outlined by Chien and Ritchie (1984). The model also tended to give higher strain values for the bottom chord than those measured in the actual structure. One significant difficulty with the model was that it did not properly predict the top chord strains of the steel joist.

Lauer (1994) expanded the joist classification system previously outlined by Azmi. Lauer reported on 11 full-scale composite joist specimens that were tested for capacity, deflection, ductility and failure mode. He sought to analyze the strength of the composite joists with various degrees of shear connection and classify them. Spans ranged from 20 ft to 40 ft and joist depths ranged from 8 in. to 20 in. Six different types of shear connector were investigated. The specimens were found to range from 27% to 149% in their ratio

of calculated shear connector capacity to measured bottom chord yield force. This ratio indicated whether the specimen was under-connected or over-connected based on a value of 100% representing a "balanced" condition.

Lauer modified Azmi's original three-category classification system by considering the involvement of forces in the top chord. To properly categorize the joists, the horizontal shear transfer capacity, along with the top chord capacity, had to be accurately known. Lauer also postulated that the shape of the load-deflection plot could be linked to the failure mode of the joist. If the plot showed a well defined yield plateau, then bottom chord yielding was likely to control. If the plot was rounded, then the joist would exhibit partial composite action and failure would be governed by top chord failure. Also, top chord performance could be linked to the amount of shear connection provided. For example, a severely under-connected joist would significantly utilize the top chord to resist applied loads, meaning that the percentage of composite action was very low.

Recent work in the United States has resulted in a proposed specification (*Proposed* 1996) on the design of composite joists and trusses. The design criteria included in this specification draw heavily from the material previously discussed. It establishes the basic considerations for composite joist and truss design procedures and provides a detailed design example demonstrating the critical aspects of the process.

1.2.2 Stub-Girder Research

Colaco (1972) first introduced the concept of the stub-girder as a unique support system designed for a specific application. He described a system using wide-flange beams that provided access for mechanical systems. Traditionally, such access had to be provided by passing conduits and ducts beneath the beams (increasing floor-to-floor heights) or by making costly web penetrations in the beams and girders. Colaco's solution was to use short beams, or "stubs," on top of the supporting girders to provide segments along the span which would be in contact with the deck and could be used to create composite action. The resulting configuration performed as a truss, where the supporting girder acted as the bottom chord, the stubs acted as web members and the slab acted as the top chord.

Wang and Gotschall (1980) noted that in the years following Colaco's presentation of stub-girders, only a few major buildings used the concept. Design firms did not have the knowledge or analysis tools to carry out the necessary design engineering. As a result, Wang and Gotschall sought to provide simple methods of analysis of stub-girder systems by investigating the most significant factors controlling their behavior.

Three models were presented. A non-prismatic beam model could be analyzed very simply using numerical integration by considering the system to be a variable cross-section beam. Only flexural stresses could be considered, however, which made the model dependent on the primary moment, and did not account for axial effects and secondary moments.

A Vierendeel truss model and a finite element model were also considered. The Vierendeel truss model was much more accurate than the non-prismatic beam because it included the effects of axial forces and their resulting deformations. It was also able to predict the stub stresses, which were necessary in designing any needed stiffeners. The finite element model could make some improvement over the Vierendeel truss, but the accuracies of both were controlled by how well the models approximate the behavior of the real system.

The authors established several important parameters in the analysis and design of stub-girder systems. The stub-girder stiffness ratio was defined as the ratio of the stiffness of the stub to the stiffness of the main girder. The overall effect of varying the stub stiffnesses was judged to be negligible, even though high stub stiffnesses might result in lower concrete and girder stresses in the vicinity of the stub. Another factor was the stub-girder length ratio; the length of each stub relative to the overall girder length. Results showed that longer stubs produced decreases in stresses and deflections throughout the system. Thirdly, the stub length ratio was the relationship of the length of the exterior stubs to the interior ones. For small stub lengths, the ratio could indicate an effect on the stresses in the girder and concrete by the stubs. As the stub lengths increased, the stubs seemed to have less of an influence on the system stress distributions.

Bjorhovde and Zimmerman (1980) reported on a research project that sought to address a number of questions that had arisen regarding stub-girders. A four-stage investigation was performed. First, a detailed analysis and design were performed for a full-size stub-girder as well as for several isolated stub specimens, which resembled push-out tests. The second stage was actual testing of the stub specimens. Thirdly, the full-size stub-girder was fabricated and tested. Finally, the test data was analyzed and correlated with the design.

A Vierendeel truss approach was employed for the preliminary analysis and design process. Once the full-size stub-girder had been designed, a series of five slab-stub specimens were constructed and tested to observe the behavior of an exterior stub with regard to various stiffening configurations. Partial end-plate stiffeners at both ends of the stub performed well without being difficult to fabricate. As a result, they were chosen for use on the full-size specimen.

The resulting full-size test was composed of a W12x58 girder with W16x26 stubs and floor beams. A total span of 44 ft was divided evenly into four spaces by three beam lines. The slab was composed of 3 in. deep fluted sheeting that supported 3.5 in. of concrete cover. Double rows of studs were used over every stub. The exterior stubs had 15 pairs of shear studs while only 5 pairs were needed over the interior stubs. The overall width of the specimen was slightly less than 9 ft.

Partial end-plate stiffeners were recommended for use on the exterior stubs because they provided as much added strength as fitted stiffeners but were more cost effective to install. Stiffeners were not provided for the interior stubs because of a lack of significant stresses measured in the interior stubs. Slab reinforcement was considered to

be an important issue, especially in the transverse direction, because the final failure of the specimens was caused by a combination of longitudinal and transverse slab cracking. The method of shear connector design, established according to Canadian guidelines, appeared to be conservative because no problems were observed to be associated with the shear studs. The application of composite design procedures to stub-girder systems seemed to give reasonable results. Thus the Vierendeel truss approach was found to model the stub-girder satisfactorily.

Buckner et al. (1981) reported that the results of testing on a stub-girder system indicated that the longitudinal slab shear strength might be the controlling factor in the shear transfer mechanism for stub-girders. The writers sought to call attention to the fact that American specifications did not have requirements for minimum areas of transverse reinforcement. This concept was of significant concern due to three "trends." First, the use of stub-girders shortened the length of slab available for shear transfer. Secondly, lightweight concrete resulted in thinner slabs and lower unit shear strengths. Concern was greatest, however, for terminal spans (where the slab would be free along one transverse edge). The writers offered a series of design recommendations that could be used in the absence of formal code requirements.

Rongoe (1984) described a system similar to the stub-girder several years later. A wide-flange girder was being used to support open-web joists. To make the girder composite, tee stub connectors were welded to the top flange between the joist seats. The girder spanned 20 ft and had six intermediate load points where the joists framed in. WT2.5x8 sections were selected for the seven stub connectors needed. The two end stubs were 18 in. long while the five interior stubs were each 12 in. long. The shear connectors were all 0.75 in. diameter headed shear studs. The slab was 3.5 in. deep on metal decking with 0.56 in. corrugations. A layer of wire mesh was the only slab reinforcement provided.

Two load test cycles were performed. Load was applied first until the estimated service loading was achieved, and then again until either twice the service load was reached or failure occurred. The specimen was found to behave elastically during the first test. The second test was able to reach the target load of twice the service load, but was showing inelastic behavior. Composite action appeared to be maintained throughout the testing. No localized yielding was observed in the girder. Analysis was performed using a Vierendeel approach. The experimental measurements showed that the system was stiffer than the theoretical predictions.

Chien and Ritchie (1984) included a chapter on stub-girders in their composite design text. They consolidated information gathered on early construction projects throughout North America using this system along with knowledge gained through participation in numerous Canadian research projects. The result was a detailed proposal of design guidelines for the complete design of a stub-girder. They also provided a rigorous floor design example for illustration.

1.2.3 Haunched Girder Research

Very little research has been conducted on haunched girder systems. Some recent work has focused on the concept of shear transfer in the system. Oehlers (1994) noted that the use of haunches has been increasing because it allows variations between the slab and beam elevations. It can also increase girder strength due to the increase in concrete depth. These aspects are balanced by the fact that the haunch causes a restriction in the side cover of shear connectors, meaning that this slab region is susceptible to splitting failures that might reduce the strength of the girder. The author reported on testing performed on nine push specimens that varied the angle of the sloping sides of the haunch. The strength of the specimens ranged from 45% to 71% of the theoretical maximum connector strength based on concrete and shear stud material properties.

1.3 Scope of Research

This research had two primary purposes. First, the research was designed to test the performances of three different methods of connecting the slabs and joist-girder top chords in order to generate composite action. Second, the research would help determine whether the current design criteria established for composite joists would be applicable to composite joist-girders.

In addition to these purposes, testing of the flush framed girder setup was designed to investigate several other issues. Would a flush framed double angle vertical connection function well as a "rigid support?" Would two inches of lateral concrete provide sufficient cover for transverse reinforcement placed over exterior joist-girders? Also, would joist deflection cause significant rotation of the exterior girders, and if so, would this cause a problem in the structure?

This report is organized into five chapters. Introductory material about the testing and a review of pertinent literature regarding composite joists, stub girders and haunched girders is presented in Chapter 1. The overall test setups, including unique details of the individual specimens, as well as instrumentation, loading apparatus and testing procedures are described in Chapter 2. The specimen test results are presented in Chapter 3. The analytical methods employed in performing and reviewing the specimen testing are reviewed in Chapter 4. A summary of the test results, conclusions and recommendations for future research are given in Chapter 5.

Sample calculations and summary material regarding the various specimens and tests can be found in the appendices. Detailed test results including load cell, strain gage, slip gage and displacement readings for the girders of each setup are presented in the appendices of the project reports (Kigudde, et al 1998; Showalter, et al 1999a; Showalter, et al 1999b).

CHAPTER II
EXPERIMENTAL SETUP

2.1 General

The specimens tested and reported on herein consisted of composite open-web steel joists and composite joist-girders. A specific orientation was established in the laboratory so that the components of the specimens could be easily referenced. In an end view or cross-section, left refers to the south side of the specimens and right refers to the north side. In a profile view, left refers to the west end of the specimens while right refers to the east end. This orientation is depicted in Figure 2.1.

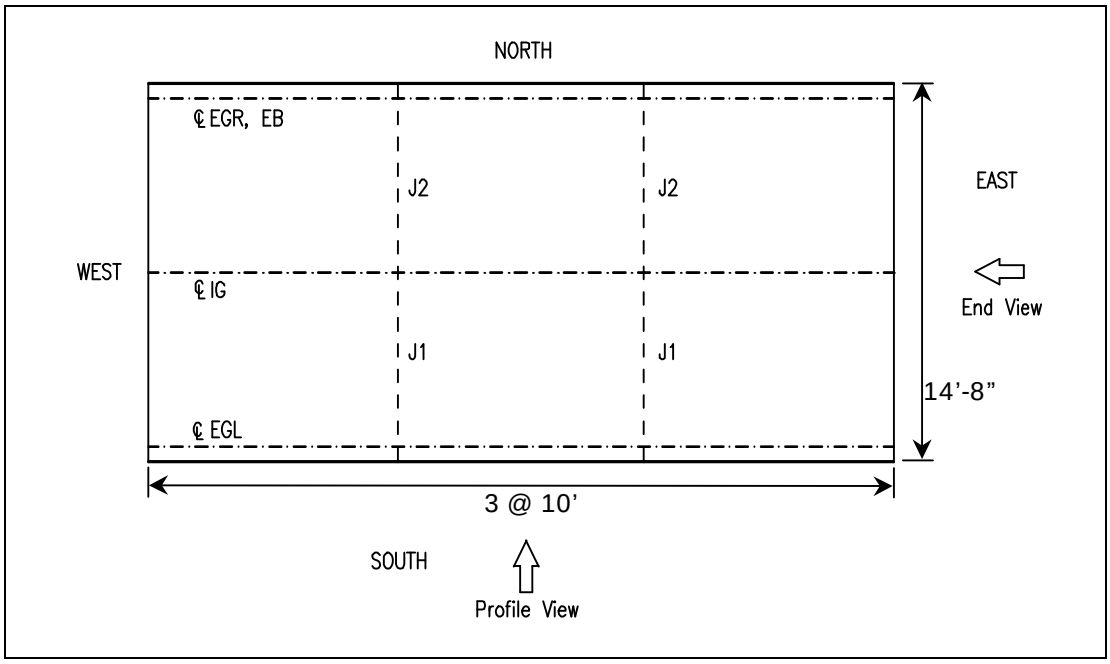

Figure 2.1 Plan View of Specimens

The exterior girders are designated "EGL" for the exterior girder (left) and "EGR" for the exterior girder (right). The interior girder is denoted as "IG." For the haunched girder setup, a wide flange beam, "EB," replaced EGR. The joists are labeled as "J1" and "J2," depending on their locations. Joists J1 span between EGL and IG while joists J2 span between IG and EGR (or EB). The joist and joist-girder locations are all indicated in Figure 2.1. The results of the tests on EB are not presented in this report, but do appear in the project report (Showalter, et. al, 1999b).

For each joist-girder (Figure 2.2), the top chord is referred to as "TC" while the bottom chord is referred to as "BC." Diagonal web members are labeled with a "W"

followed by a number starting with 2 at the west end and increasing by 1 toward midspan. The diagonal web members on the opposite side follow the same numbering sequence, but an "R" is added at the end of the label, e.g. W2R. For the flush framed setup, two additional diagonal members were used near each end, W2DL and W2DR.

This numbering sequence means that all tension members are even numbered and all compression members are odd numbered. The vertical web members are labeled with "V" followed by a number starting with 1 at the left end and increasing by 1 to the opposite end. The joist members are identified similarly to the girders and are shown in Figure 2.3.

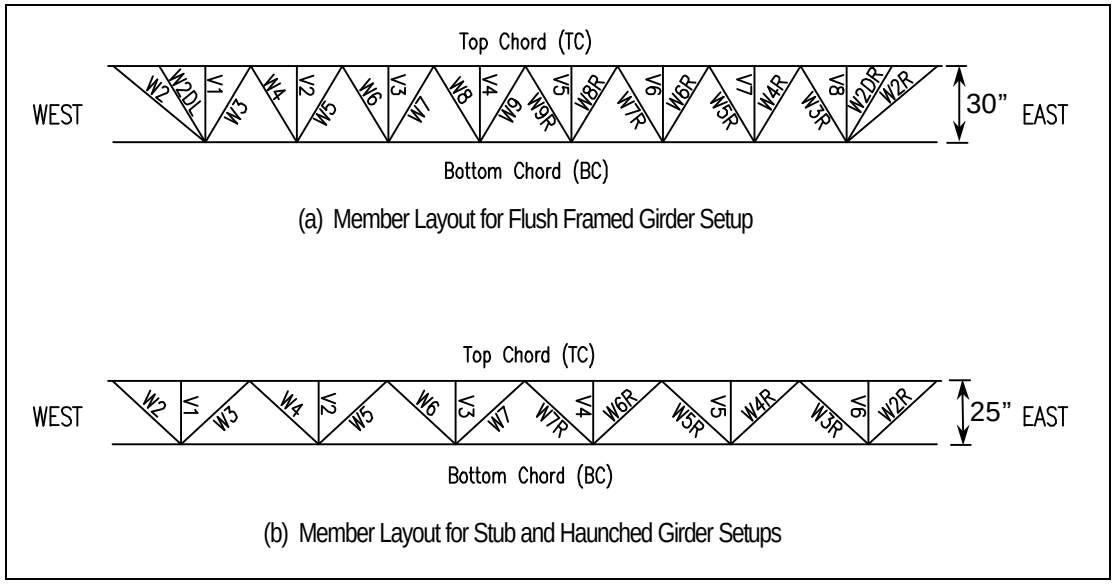

Figure 2.2 Joist-Girder Member Nomenclature

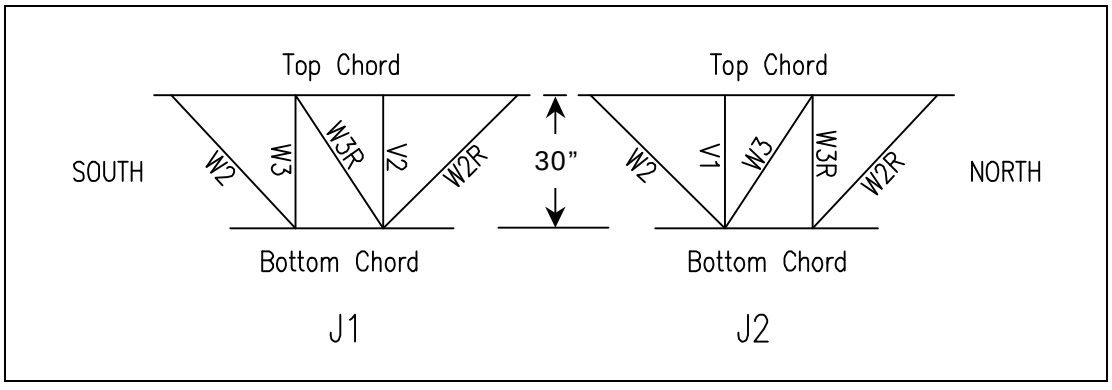

Figure 2.3 Joist Member Nomenclature

The specimens tested were designed to simulate two-bay floor systems. Three joist-girders were used to establish the two bays (EGL, IG, EGR). Two equally spaced joists (J1, J2), shown previously in Figure 2.1, spanned between each joist-girder. The joist-girders all used modified Warren configurations and spanned 30 ft. The flush framed girders were 30 in. deep while the stub girders and haunched girders were 25 in. deep. The joists were limited to approximately 7 ft in length so that an overall setup width of 14 ft 8 in. could be maintained to accommodate erection of the laboratory load frames. For all three specimens, the joists were 30 in. deep and were located at the third points of the joist-girder spans. The overall lengths of the joists depended on which specimen they were part of and how they were being connected to their supporting joist-girders.

The specimens all used 18 gage Vulcraft 2VL steel deck cut to 30 ft 4 in. lengths. Channels were positioned between the girder seats to support the ends of the deck sheets. The 2 in. deep deck supported a normal weight concrete slab having a cover depth of 3 in., giving a total slab depth of 5 in. For the haunched girder specimen, concrete haunches were formed over the joist girders for an additional depth of 5 in. so that the slab thickness directly over the joist girders was 10 in. In all cases, the girders were supported by load cells positioned on support stands at the east and west ends of the specimens. The girder bottom chords were stabilized at their ends by extending the chords on either side of 0.75 in. x 8 in. x 8 in. stabilizer plates, shown in Figure 2.1, which were attached to the support stand rafters. These stabilizer plates also acted as flange stiffeners for the support stand rafters at the load points.

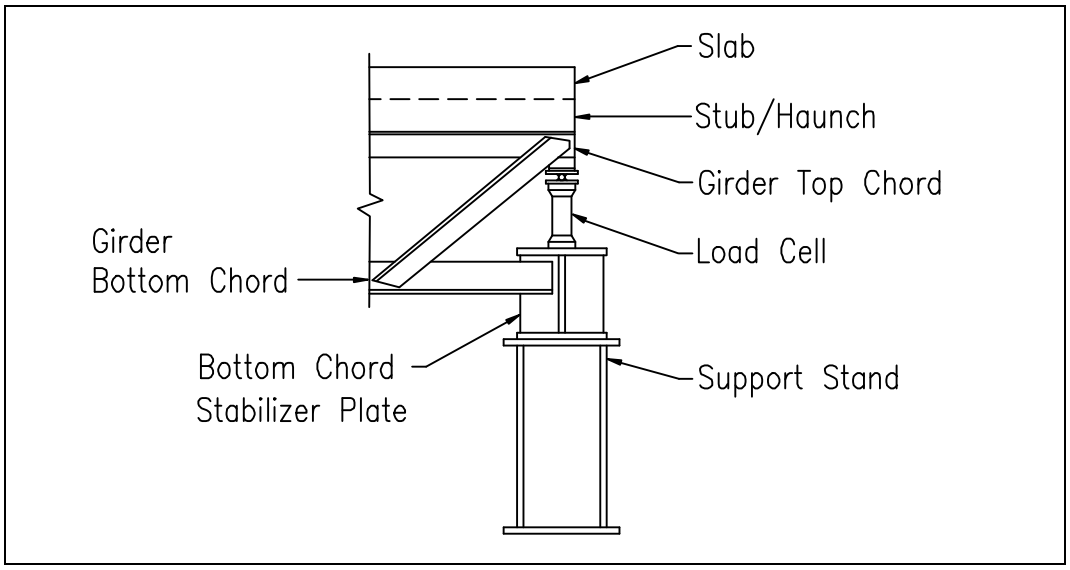

Figure 2.4 Girder End Support Detail

2.2 Construction Details

All open-web joists and joist-girders were fabricated by Vulcraft and shipped to the Structures and Materials Research Laboratory at Virginia Tech. Once at the lab, the joists and joist-girders were inspected and the joist-girders were instrumented with strain gages. The joist-girders were placed in position on the support stands, and the joists were then erected on the joist-girders. Next, the steel deck was laid out and positioned over the joists and channels, with the ribs parallel to the joist-girders. Cold-formed steel pourstop was installed around the perimeter of the floor and was left in place for the duration of testing. Stud locations were marked on the deck and 0.75 in. diameter headed shear studs were welded to the joists and joist-girders.

One layer of welded wire fabric (WWF6x6-W2.1x2.1) was prepared and put in place for shrinkage control. Transverse reinforcement was also installed over the joist-girders to provide longitudinal shear resistance in the slab. Holes were drilled through the steel deck adjacent to the first and second panels of each girder end to be used later when connecting slip gages to the slab. The holes were covered with tape to prevent wet concrete from spilling through during placement.

The joist-girders were instrumented with all measuring devices except slip gages prior to concrete placement. The data acquisition systems were zeroed just prior to concrete placement. The concrete was placed from the east end to the west end. Cylinders were cast along with the slab so that concrete compressive strength tests could be performed during the slab curing period. Once the slab had been placed and the surface finished, measurements were taken again for all recording devices. The slab was then covered with plastic for seven days, during which time water was applied to the surface daily. The plastic was removed after seven days and the slab was air cured until the specimen was tested.

2.2.1 Flush Framed Girder Specimen

For this specimen, girders measuring 30 in. deep and 30 ft 4 in. long were used. The top chord panel points were spaced at 1 ft 8 in. The nominal member sizes for the joist-girders and joists are given in Tables 2.1 and 2.2.

Table 2.1 Flush Framed Girder Specimen – Nominal Girder Member Sizes

MEMBER	NOMINAL SIZE	
	EGL and EGR	IG
Top Chord	2L-3.00x3.00x0.250	2L-4.00x4.00x0.375
Bottom Chord	2L-4.00x4.00x0.375	2L-5.00x5.00x0.625
W2, W2R	2L-3.00x3.00x0.250	2L-4.00x4.00x0.375
W2DL, W2DR	1L-2.00x2.00x0.187	2L-1.75x1.75x0.170
V1,V8	1L-1.75x1.75x0.155	1L-2.00x2.00x0.250
W3, W3R	2L-2.50x2.50x0.250	2L-3.50x3.50x0.344
W4, W4R	2L-2.50x2.50x0.212	2L-3.50x3.50x0.344
V2, V7	1L-1.75x1.75x0.155	1L-2.00x2.00x0.250
W5, W5R	2L-2.50x2.50x0.250	2L-3.50x3.50x0.344
W6, W6R	2L-2.50x2.50x0.212	2L-3.50x3.50x0.375
V3, V6	2L-5.00x5.00x0.438	2L-4.00x4.00x0.500
W7, W7R	2L-1.50x1.50x0.155	2L-2.00x2.00x0.176
W8, W8R	2L-1.25x1.25x0.133	2L-1.50x1.50x0.170
V4, V5	1L-1.75x1.75x0.155	1L-2.00x2.00x0.250
W9, W9R	2L-1.50x1.50x0.138	2L-2.00x2.00x0.176

Table 2.2 Flush Framed Girder Specimen – Nominal Joist Member Sizes

	MEMBER	NOMINAL SIZE		MEMBER	NOMINAL SIZE
J1	Top Chord	2L-3.00x3.00x0.313	J2	Top Chord	2L-3.00x3.00x0.313
	Bottom Chord	2L-4.00x4.00x0.500		Bottom Chord	2L-4.00x4.00x0.500
	W2	2L-3.50x3.50x0.344		W2	2L-3.50x3.50x0.344
	W3	2L-3.00x3.00x0.313		V1	2L-3.50x3.50x0.375
	W3R	2L-2.50x2.50x0.250		W3	2L-2.50x2.50x0.250
	V2	2L-3.50x3.50x0.375		W3R	2L-3.00x3.00x0.313
	W2R	2L-3.50x3.50x0.344		W2R	2L-3.50x3.50x0.344

The four joists spanned 7 ft between girder centerlines. They framed into the joist-girders using bolted connections with special vertical web members, V3 and V6, at the joist-girder span third points. These connections were made with either 3 or 4 bolts through 1 in. x 9 in. x 12 in. knife plates attached to the joist ends and through the special double angle vertical web members of the joist-girders. The connections to EGL and IG for the joists J1 used 3 bolts each while the connections for the joists J2 were 3-bolt to IG and 4-bolt to EGR.

A 9/16 in. diameter rod was welded at one end to the bottom chord of EGL at each third point and to the adjacent joist bottom chord at the other end. This was to prevent the bottom chord of EGL from moving laterally. No rods were attached to EGR so that a comparison of behavior between the two girders could be made. Also, the 3-bolt

connections to IG were designed as “rigid” single plate framing connections. The 3-bolt connections to EGL were to act as rigid connections in conjunction with the bottom chord braces. The 4-bolt connections to EGR were designed as flexible connections.

A cross-section of the specimen near a joist line is depicted in Figure 2.5, showing the deck centered over the joist-girders and the joist positions in relation to those joist-girders.

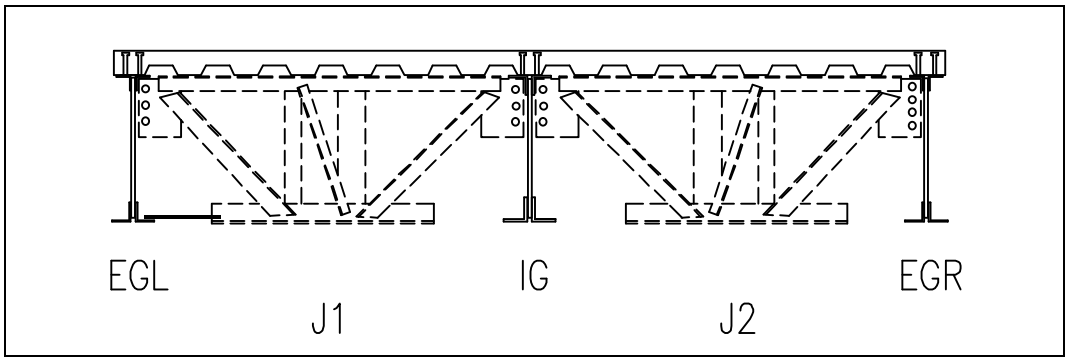

Figure 2.5 Flush Framed Girder Specimen Cross-Section

The ends of the deck sheets, at the east and west ends of the specimen, were supported by 76 in. long channels (C6x10.5) which spanned between the joist-girder ends and were welded to the joist-girder seats. Headed shear studs were installed in staggered double rows along the joist-girder top chords and in uniform double rows along the joists. A total of 56 studs were welded to IG, 30 to EGL, 30 to EGR, and 24 total along each joist line. All studs were 0.75 in. diameter and stood 4.5 in. after welding. The stud layout is shown in Figure 2.6. A minimum of two inches of concrete was maintained between the outer shear studs and the edge of the deck slab. Results of testing on this specimen would also be used to evaluate whether two inches of concrete provides sufficient cover to fully develop the shear studs. Transverse slab reinforcement was prepared and laid out as shown in Figure 2.7 having been designed specifically for each joist-girder.

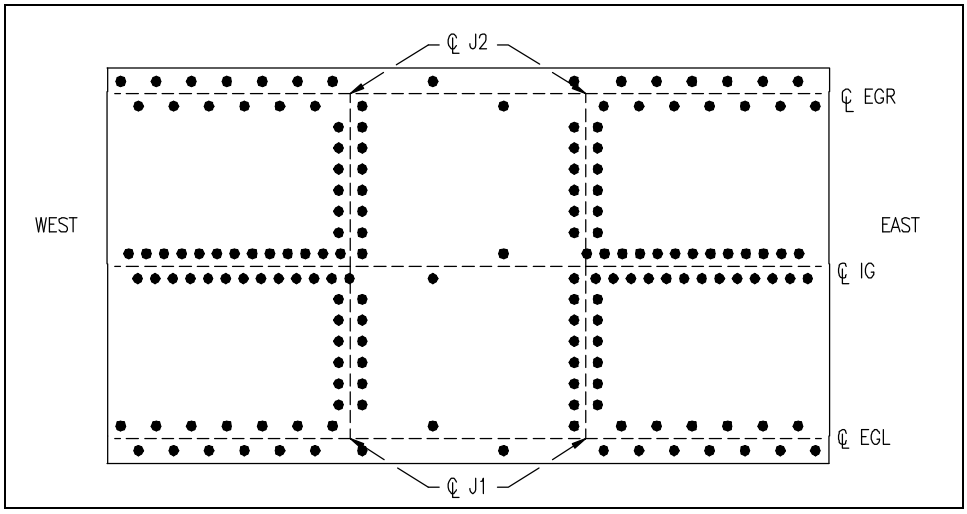

Figure 2.6 Flush Framed Girder Shear Stud Layout

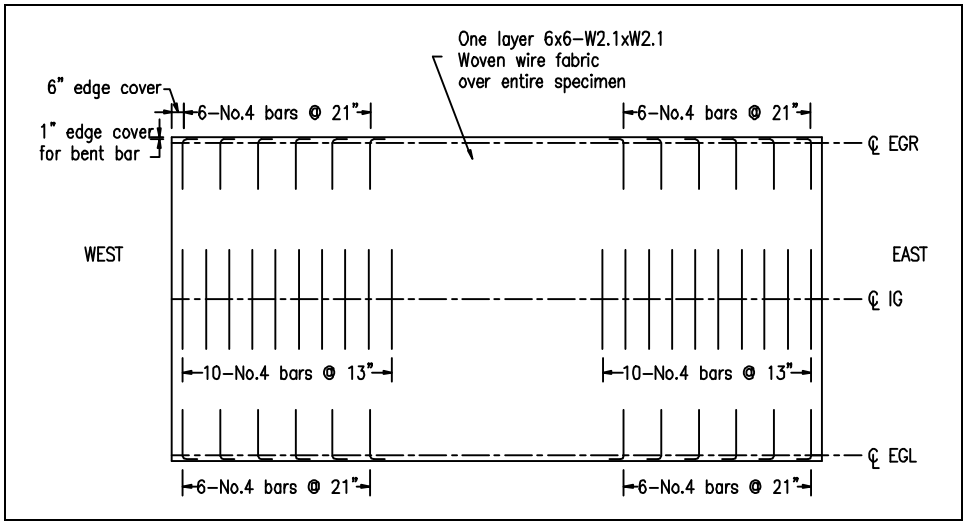

Figure 2.7 Flush Framed Girder Slab Reinforcement Layout

2.2.2 Stub-Girder Specimen

For this specimen, the joist-girders were all 25 in. deep and 30 ft 4 in. long. The top chord panel points were spaced at 2 ft 6 in. The nominal member sizes for the joist-girders and joists are given in Tables 2.3 and 2.4.

Each joist-girder had three S5x10 “stubs” attached along the length of the top chord. Gaps between the stubs at the joist-girder span third points provided 8 in. wide spaces where the joist seats would rest. The end stubs were each 116 in. long while the

center stub on each joist-girder was 112 in. long. The four joists spanned 7 ft between joist-girder centerlines and rested on the joist-girder top chords between the stubs.

Table 2.3 Stub-Girder Specimen – Nominal Girder Member Sizes

MEMBER	NOMINAL SIZE	
	EGL and EGR	IG
Top Chord	2L-3.00x3.00x0.250	2L-4.00x4.00x0.375
Bottom Chord	2L-4.00x4.00x0.375	2L-5.00x5.00x0.625
W2, W2R	2L-3.00x3.00x0.227	2L-4.00x4.00x0.375
V1, V6	1L-1.50x1.50x0.155	2L-1.50x1.50x0.155
W3, W3R	2L-3.00x3.00x0.281	2L-4.00x4.00x0.438
W4, W4R	2L-3.00x3.00x0.227	2L-4.00x4.00x0.375
V2, V5	1L-1.50x1.50x0.155	2L-1.50x1.50x0.155
W5, W5R	2L-3.00x3.00x0.281	2L-4.00x4.00x0.438
W6, W6R	2L-1.50x1.50x0.155	2L-2.00x2.00x0.205
V3, V4	1L-1.50x1.50x0.155	2L-1.50x1.50x0.155
W7, W7R	2L-1.75x1.75x0.155	2L-2.00x2.00x0.232
Stubs	S5x10	S5x10

Table 2.4 Stub-Girder Specimen – Nominal Joist Member Sizes

	MEMBER	NOMINAL SIZE		MEMBER	NOMINAL SIZE
J1	Top Chord	2L-3.00x3.00x0.313	J2	Top Chord	2L-3.00x3.00x0.313
	Bottom Chord	2L-4.00x4.00x0.500		Bottom Chord	2L-4.00x4.00x0.500
	W2	2L-3.50x3.50x0.375		W2	2L-3.50x3.50x0.375
	W3	2L-3.00x3.00x0.250		V1	2L-3.50x3.50x0.375
	W3R	2L-3.00x3.00x0.281		W3	2L-3.00x3.00x0.281
	V2	2L-3.50x3.50x0.375		W3R	2L-3.00x3.00x0.250
	W2R	2L-3.50x3.50x0.375		W2R	2L-3.50x3.50x0.375

The steel deck was positioned so that it lay offset 1.56 in. from the centerline of IG (Figure 2.8). This was necessary because the narrow width of the stub top flanges required a single row of studs directly over the stub webs. As a result, the deck had to be shifted so that the stiffener in the bottom rib of the deck would not interfere with stud placement. At the ends of the specimen, the deck sheets were again supported by 76 in. long channels (C10x15.3). Headed shear studs were installed in single rows over each stub, and in double rows along each joist top chord. In all, 56 studs were welded to IG, 28 to EGL, 28 to EGR and 30 along each joist line. All studs were 0.75 in. diameter and stood 4.5 in. after welding. Stud layout is shown in Figure 2.9.

Transverse slab reinforcement for each joist-girder was prepared and laid out as shown in Figure 2.10. The reinforcement required for each joist-girder was designed by David Samuelson, Nucor Research & Development, based on an analysis of shear stresses in the slab of a stub girder presented by Buckner (Buckner 1981). Buckner recommended a limit on concrete stress in shearing planes that would, in turn, indicate the amount of transverse reinforcement needed. The amount of reinforcement over EGL and EGR varied because of the difference in width of the full depth slab over each joist-girder.

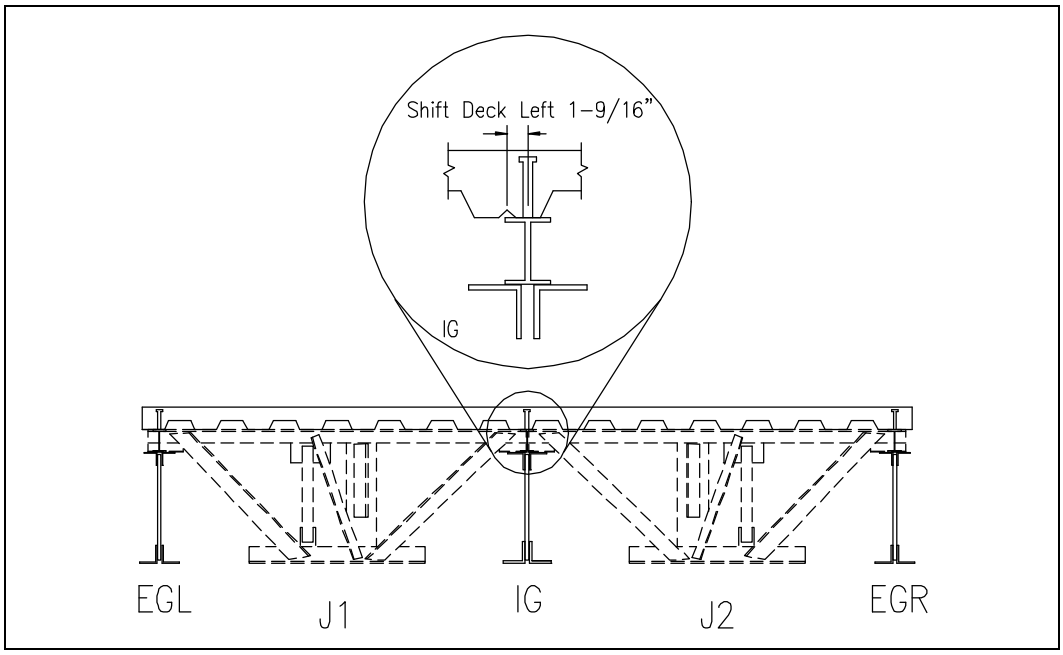

Figure 2.8 Stub-Girder Specimen Cross-Section

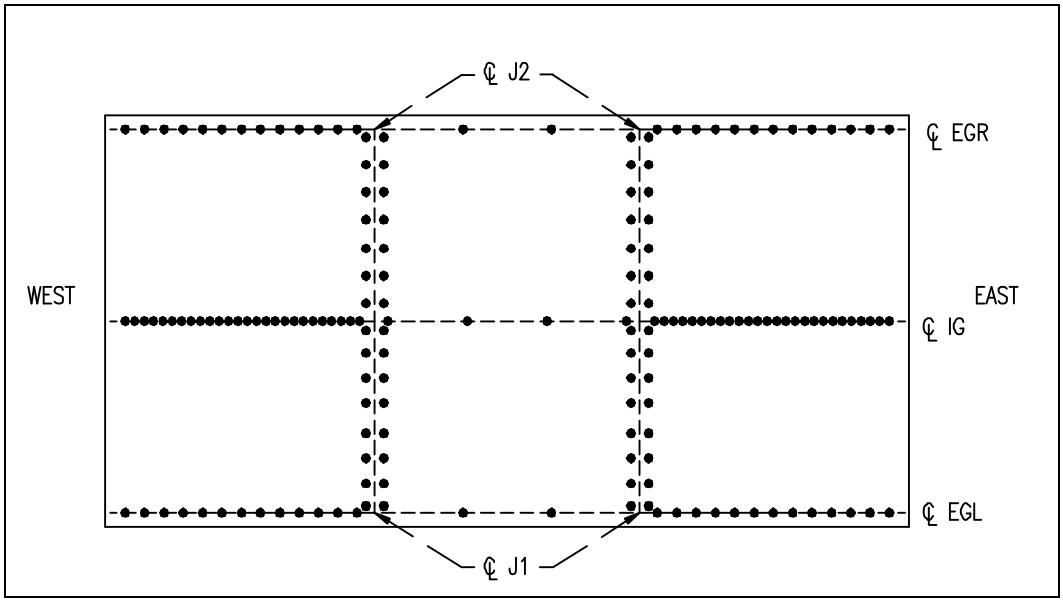

Figure 2.9 Stub-Girder Shear Stud Layout

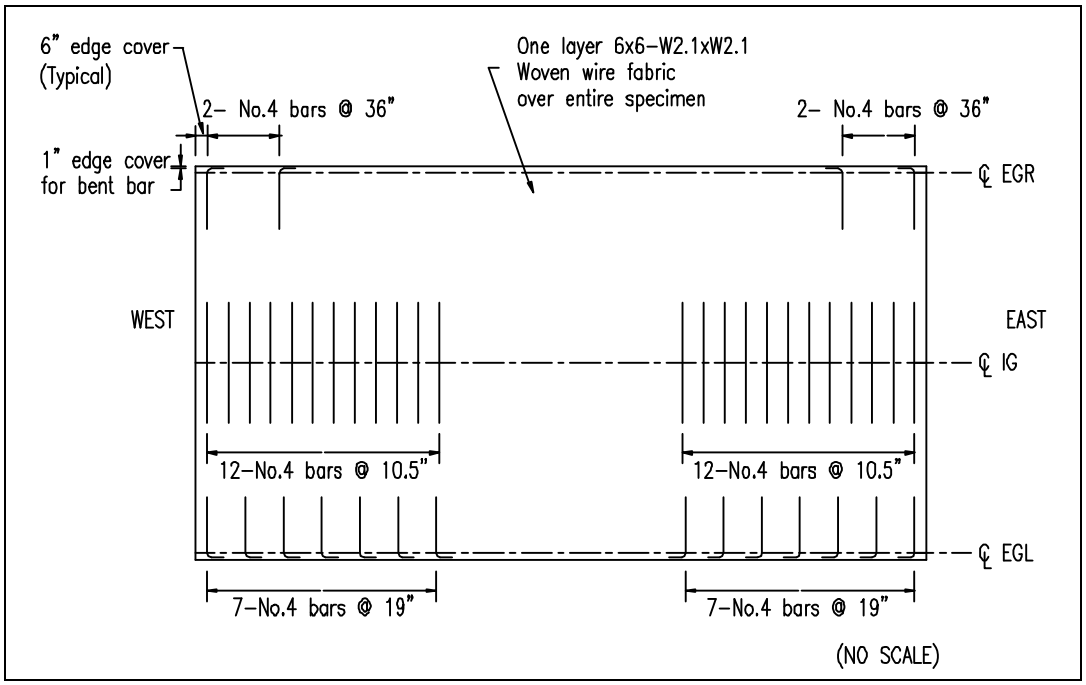

Figure 2.10 Stub-Girder Slab Reinforcement Layout

2.2.3 Haunched Girder Specimen

For this specimen, the joist-girders used were 25 in. deep and 30 ft 4 in. long. Again, the top chord panel points were spaced at 2 ft 6 in. The nominal member sizes for the joist-girders and joists are given in Tables 2.5 and 2.6.

In addition to testing the haunched configuration, this specimen was also designed to compare the performance of the joist-girders with the performance of a regular wide-flange shape. To accomplish this, one of the exterior joist-girders, EGR, was replaced with a W24x55 wide-flange beam designed to match the joist-girder capacity. The behavior of this beam will not be discussed in detail here due to the focus on joist-girder performance. The four joists connecting the joist-girders spanned 6 ft 9 in. between girder centerlines. They were seated on the joist-girder top chords and flush framed with the beam top flange.

Table 2.5 Haunched Girder Specimen – Nominal Girder Member Sizes

MEMBER	NOMINAL SIZE	
	EGL	IG
Top Chord	2L-3.00x3.00x0.250	2L-4.00x4.00x0.375
Bottom Chord	2L-4.00x4.00x0.375	2L-5.00x5.00x0.625
W2, W2R	2L-3.50x3.50x0.287	2L-4.00x4.00x0.500
V1, V6	1L-1.50x1.50x0.155	2L-1.50x1.50x0.155
W3, W3R	2L-3.50x3.50x0.313	2L-5.00x5.00x0.438
W4, W4R	2L-3.50x3.50x0.287	2L-4.00x4.00x0.500
V2, V5	1L-1.50x1.50x0.155	2L-1.50x1.50x0.155
W5, W5R	2L-3.50x3.50x0.313	2L-5.00x5.00x0.438
W6, W6R	2L-1.75x1.75x0.170	2L-2.50x2.50x0.212
V3, V4	1L-1.50x1.50x0.155	2L-1.50x1.50x0.155
W7, W7R	2L-2.00x2.00x0.176	2L-2.50x2.50x0.250

Table 2.6 Haunched Girder Specimen – Nominal Joist Member Sizes

	MEMBER	NOMINAL SIZE		MEMBER	NOMINAL SIZE
J1	Top Chord	2L-3.50x3.50x0.344	J2	Top Chord	2L-3.50x3.50x0.313
	Bottom Chord	2L-3.50x3.50x0.313		Bottom Chord	2L-3.50x3.50x0.287
	W2	2L-4.00x4.00x0.438		W2	2L-4.00x4.00x0.438
	W3	2L-3.50x3.50x0.287		V1	2L-4.00x4.00x0.375
	W3R	2L-3.50x3.50x0.344		W3	2L-3.00x3.00x0.313
	V2	2L-4.00x4.00x0.375		W3R	2L-4.00x4.00x0.375
	W2R	2L-4.00x4.00x0.375		W2R	2L-4.00x4.00x0.375

The haunches formed over the joist-girders resulted in 10 in. concrete depths. The beam was positioned so that the top flange was at the same elevation as the joist-girder top chords. Thus the slab had a solid thickness of 5 in. over the beam. Full-length deck sheets were placed over the joists first. The deck sheets were supported at the ends by 57 in. and 63 in. long channels (C10x15.3). The haunches were then constructed using cold-formed pourstop material of varying thicknesses. The haunch forms overlapped the edges of the normal deck sheets. The haunch forms were cut to fit along the third spans of the joist-girders, between the joist seats and between the joist seats and the slab end forms. Special blockouts were made to fit around the joist seat components so that they would be encased in concrete. The seats were then used as additional large shear connectors.

On the beam side of the floor setup, a piece of flat pourstop was used to bridge the gap between the outside sheet of decking and the inside edge of the beam top flange. The pourstop forming the outside slab edge along the beam was fixed to the beam top flange with puddle welds. A cross-section is shown in Figure 2.11. The slanted haunch segments were formed with 16 gage steel. The outside edge along EGL was formed with 10 gage steel. The outside edge along EB was formed with 20 gage steel.

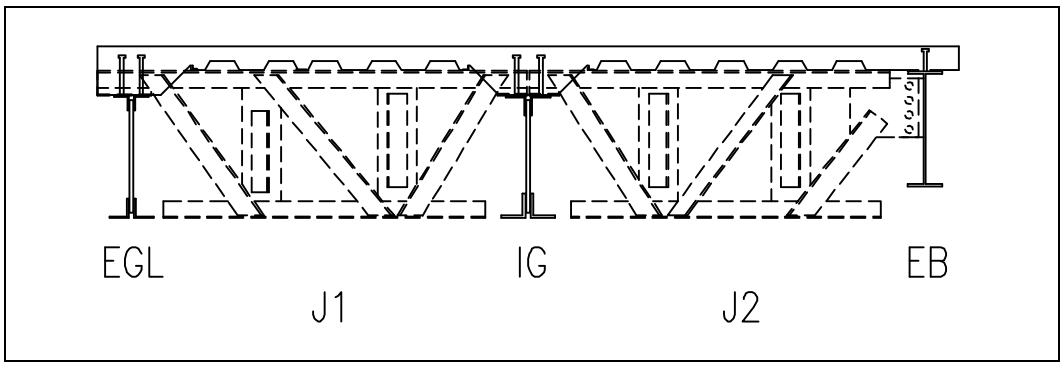

Figure 2.11 Haunched Girder Specimen Cross-Section

Headed shear studs were welded in double rows to the joists and joist-girders, and in a single row along the beam top flange. A total of 107 studs were welded to IG, 55 to EGL, 37 to EB, and 30 along each joist line. All studs were of 0.75 in. diameter. The studs used over the joists and EB stood 4.5 in. tall after welding while the studs used over EGL and IG stood 8 in. tall after welding. The haunch studs required this greater height so that the heads reached into the upper portion of the slab in the region of the haunches. The stud layout is shown in Figure 2.12.

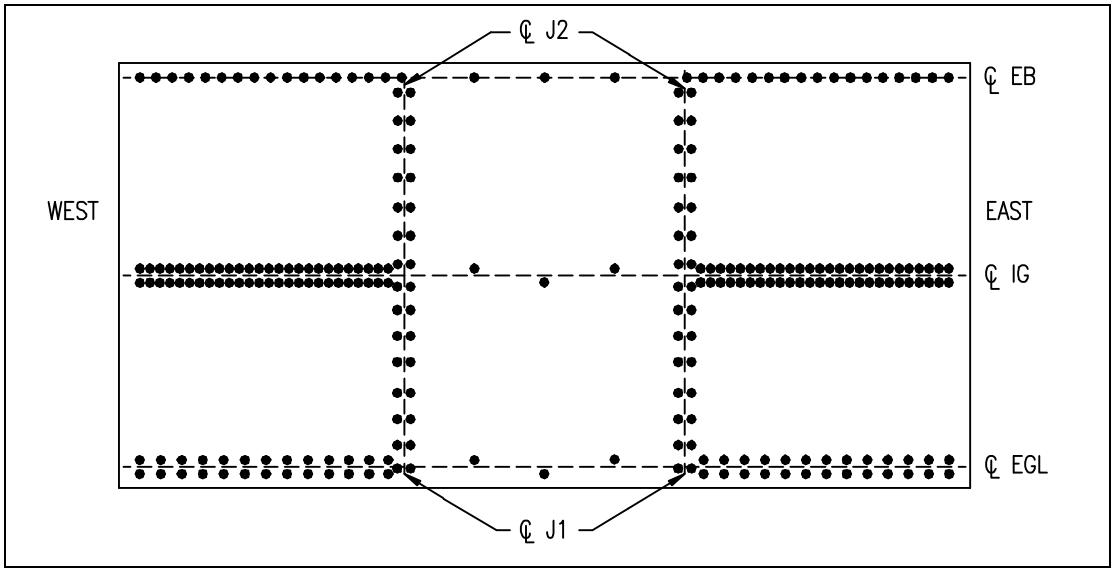

Figure 2.12 Haunched Girder Shear Stud Layout

Bent reinforcing steel was used in the haunched regions over the girders, as shown in Figure 2.13. The slab reinforcement layout is shown in Figure 2.14. Note that no transverse reinforcement was designed for placement over EB.

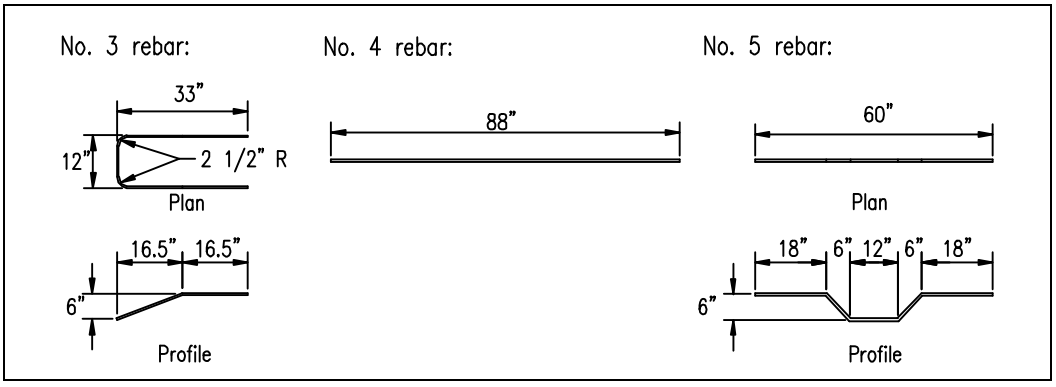

Figure 2.13 Haunched Girder Slab Reinforcement Details

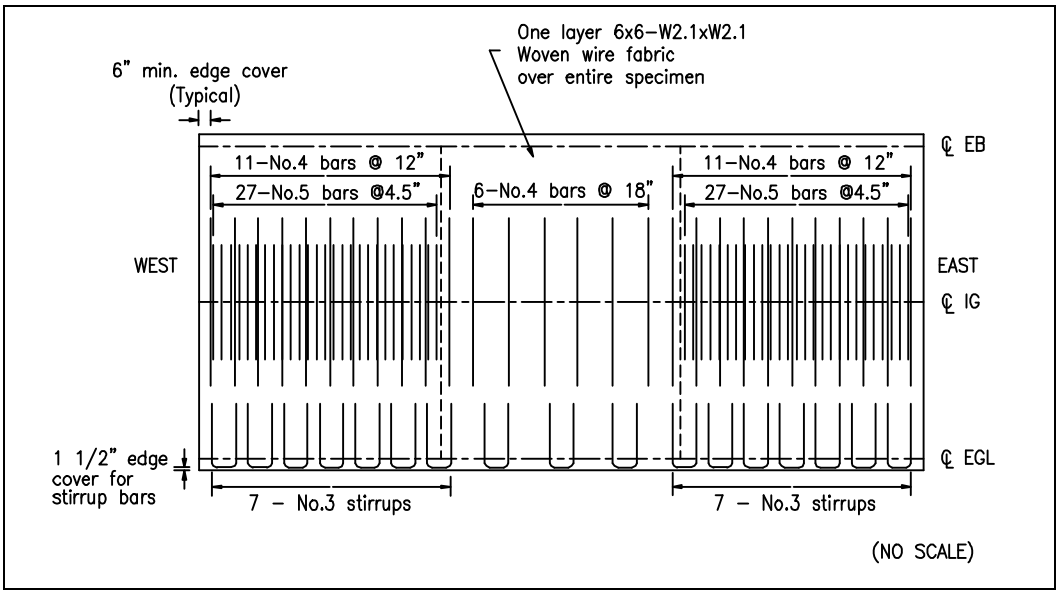

Figure 2.14 Haunched Girder Slab Reinforcement Layout

2.3 Instrumentation

The joist-girders were instrumented as shown in Figures 2.15 - 2.17. Strain gages were placed at various locations on the top and bottom chords and on selected web members. Strains in the concrete slabs were measured at midspan for all specimens and over the west third point for the stub and haunched joist-girder specimens.

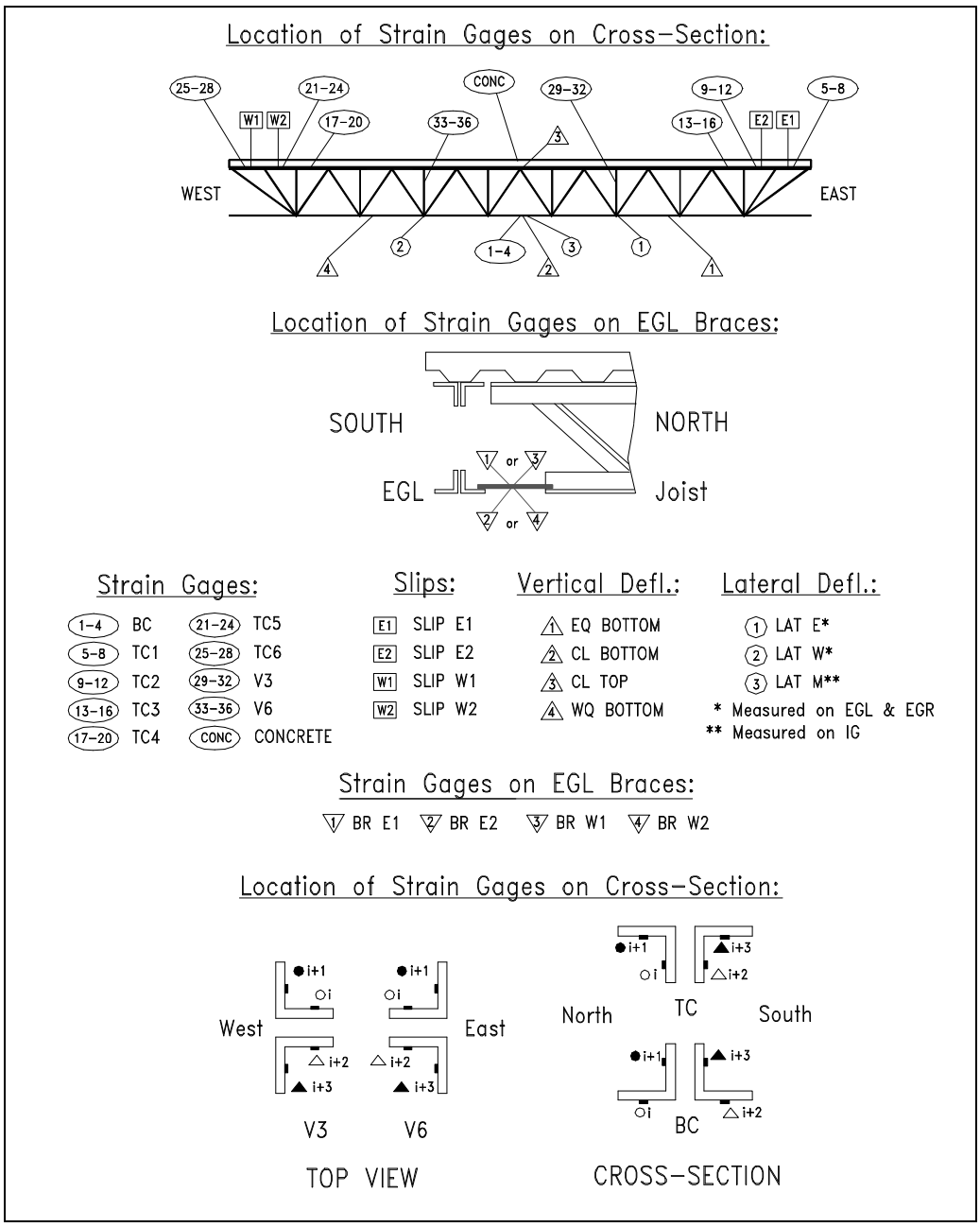

Figure 2.15 Flush Framed Girder Testing Instrumentation

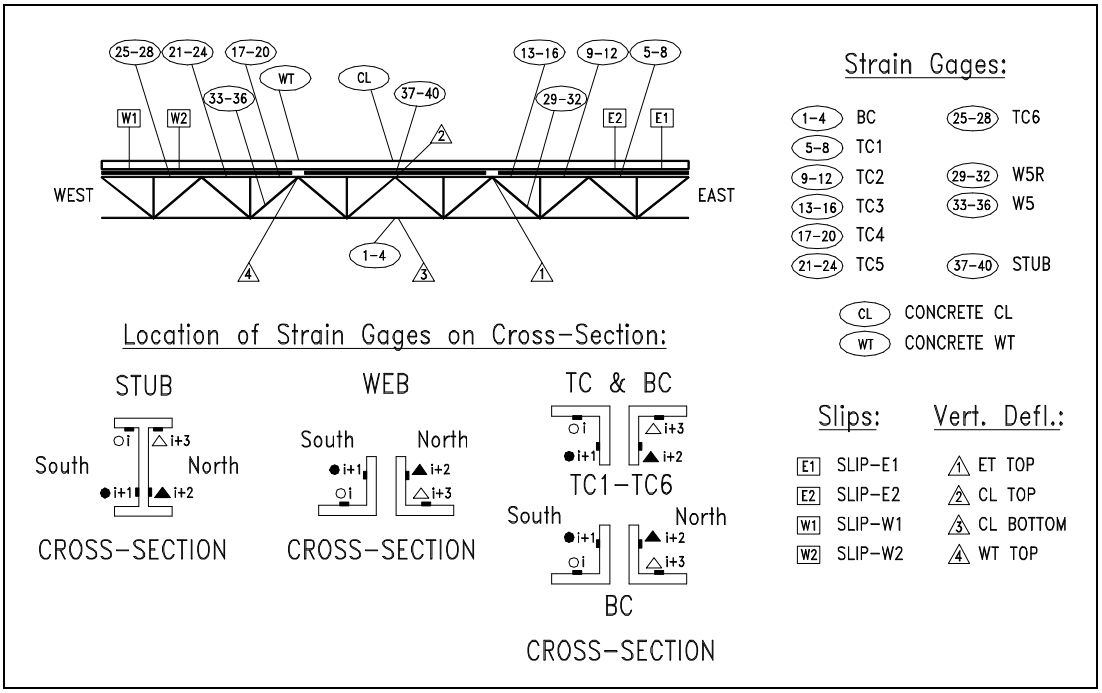

Figure 2.16 Stub-Girder Testing Instrumentation

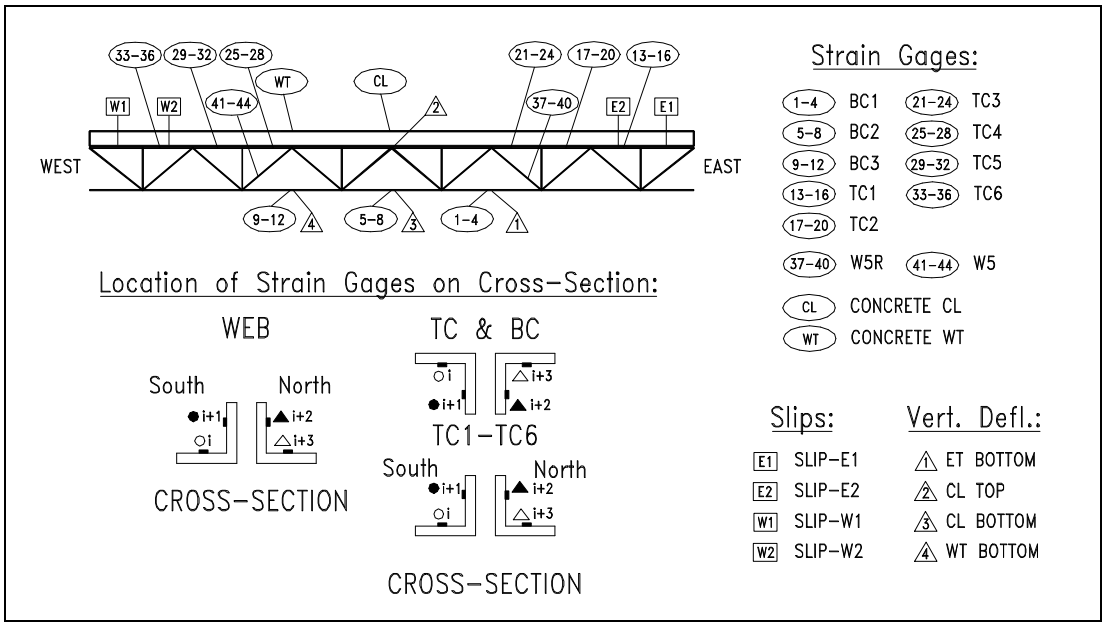

Figure 2.17 Haunched Girder Testing Instrumentation

Slip movements between joist-girder and slab were measured by linear potentiometers that were attached to nails that had been driven into the slab through the slip holes. Vertical deflections were measured using linear transducers at the midpoint and third points of each joist-girder. End reactions were measured using load cells placed under each joist-girder or beam support.

2.4 Loading Apparatus

Two hydraulic rams (400 kips capacity each) provided applied load to each floor system during testing. The rams were suspended from load frames located at the third points of the joist-girder span. The rams could be repositioned within the load frames to accommodate the requirements of the different load arrangements. The complete load frame is shown in Figure 2.18. The applied ram loads were transferred to each floor through 15 ft W27x84 load distribution beams which sat perpendicular to the joist-girders along the joist lines. These beams were braced at the ends to allow movement vertically but prevent movement laterally.

The loads were transferred from the beams to the floor by stacks of 1 in. x 6 in. x 6 in. steel plates. Two or three plates were used at each loading point. The plates could easily be moved to the different locations required by the various tests. The positions of the rams and plates for each test are described in Section 2.5.

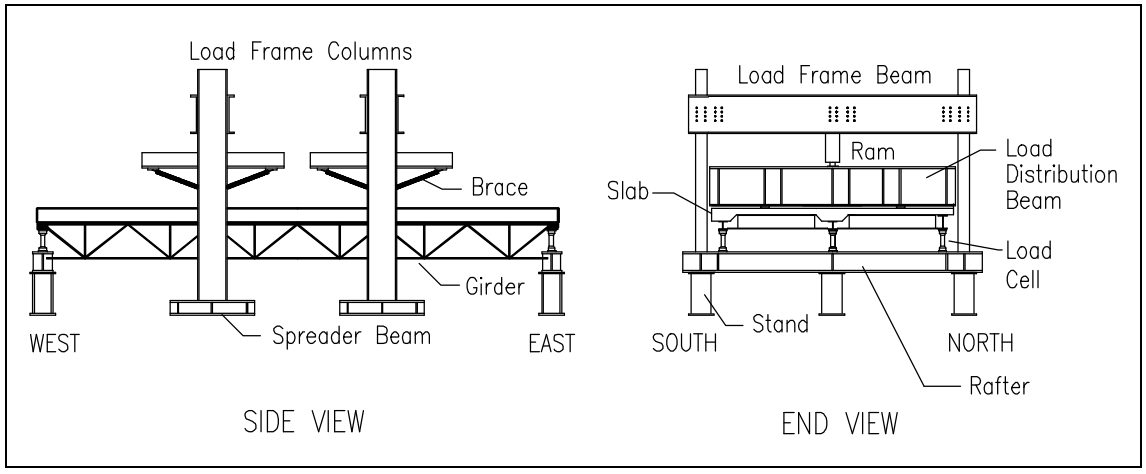

Figure 2.18 Load Frame

2.5 Testing Procedures

2.5.1 General

Once the frames and slab forms were completely installed, all measuring instruments, except slip gages, were connected to two data acquisition systems. Readings

were taken before and after placement of the concrete in order to measure the effect of the wet concrete.

Strains and vertical displacements due to the dead weight of the steel in the specimens were extrapolated from the effects of the concrete by a weight ratio. The total weight of the steel was calculated theoretically based on joist-girder and joist weights provided by Nucor Research and Development. The weight of each joist was assumed to evenly distribute to the interior and exterior joist-girder to which it was connected. Once the concrete slab had cured adequately, the load frames were assembled. All instrumentation was again organized, attached to each specimen, and zeroed. The system was then preloaded to verify that all instrumentation was working properly.

Each specimen was generally loaded in increments of 5 kips to 20 kips of joist-girder end reaction. After the desired load was reached, the specimen was unloaded. Several readings were taken during the process of unloading. The load plates and/or the rams were moved between tests to the positions required for each subsequent test. For each load increment applied or reduced, the system was allowed to stabilize before data was recorded electronically by the data acquisition systems. Selected data was entered into a spreadsheet to generate plots of various relationships such as applied load versus bottom chord deflections, applied load vs. bottom chord strains, applied load vs. compression web strains, and applied load vs. slip during the tests in order to monitor behavior. After the applied load vs. deflection curves no longer showed linear elastic behavior, displacement control was used for the remainder of the test.

2.5.2 Flush Framed Girder Tests

The load configurations for the flush framed joist-girder tests are shown in Figure 2.19. For the first loading, the load points were placed 4 ft on either side of IG. The load was increased in 5 k increments in order to reach the nominal service load of 46.9 k at each end reaction of EGL and EGR. The total load reported included self-weight of the joist-girder, joists, deck and slab, as well as the applied load. The specimen was then unloaded.

For the second loading, the load points were moved to a distance of 3 ft on either side of IG. Load was applied in 10 k increments to reach the service load of 94.5 k at the ends of IG. The specimen was then unloaded.

The third loading used the same setup as the second. Load was increased in 20 k increments, then by lesser increments, in order to reach the yield load in IG. The specimen was then unloaded.

The fourth loading repeated the setup and load points used in the first. Load was applied in 20 k increments until the yield load was reached for EGL and EGR. Beginning with this test, and for all subsequent tests, dial gages were used to measure the lateral displacements of the exterior joist-girder bottom chords at the span third points.

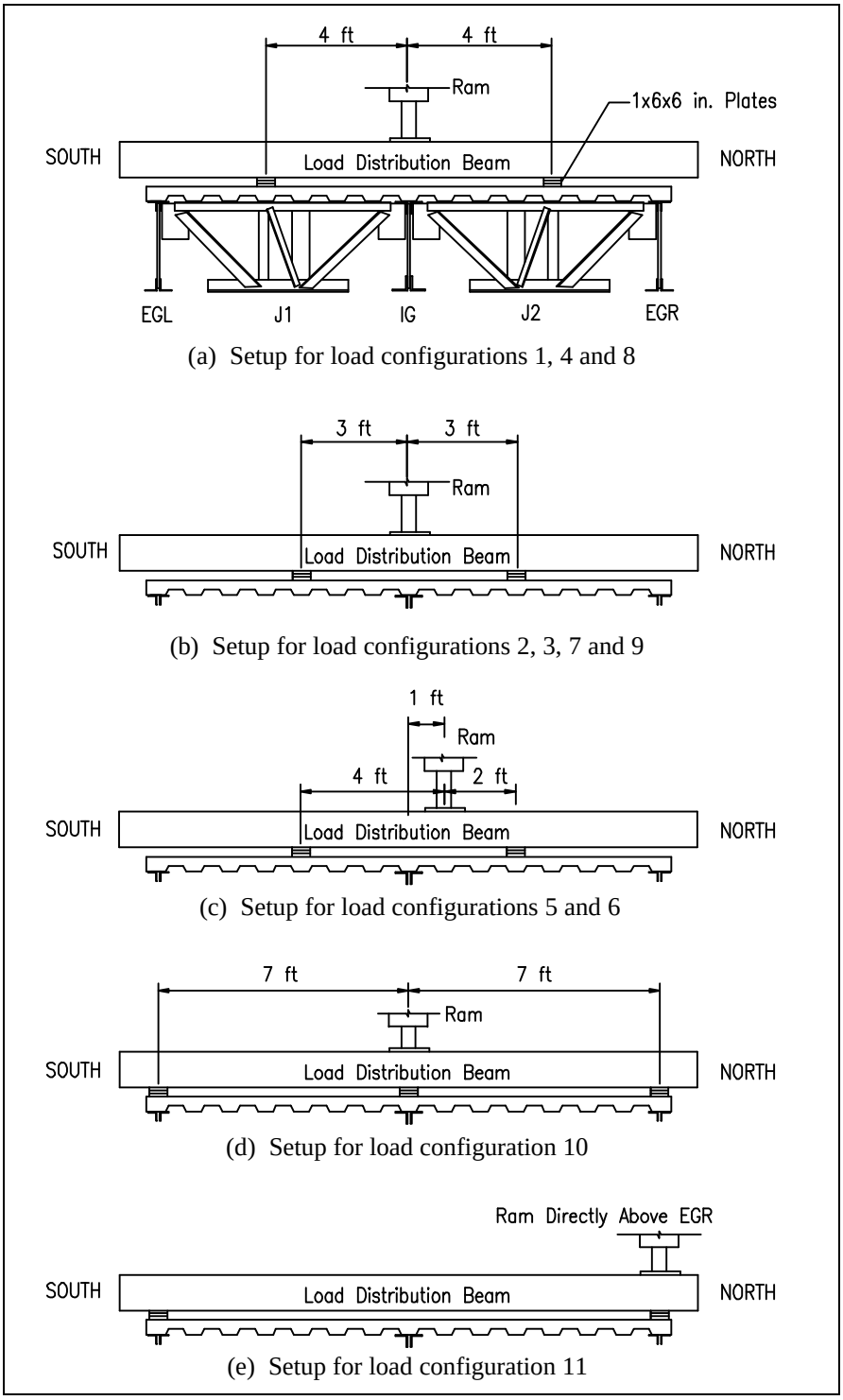

Figure 2.19 Flush Framed Girder Load Configurations

In the fifth loading, the load points were returned to 3 ft on either side of IG. The rams were also moved 1 ft toward EGR in the load frames so that an uneven load could be applied to the interior joist-girder. This was to simulate a composite live load of 73 psf and dead load of 37 psf on one side of IG while only the dead load of 37 psf would be applied to the other side. Load was applied in 10 k increments until an unbalanced service load of 67.8 k was reached at each reaction of IG. For this, and all subsequent loadings, a transducer was connected to the bottom chord of IG to monitor lateral displacement.

The sixth loading repeated the setup of the fifth, but load was applied in 20 k increments until the anticipated unbalanced yield load, approximately 111 k, was achieved at each end of IG.

The seventh loading used the same setup as was used for the second. Load was applied in 20 k increments until the applied load vs. midspan deflection curve for IG became significantly non-linear. After this, load was applied in 0.25 in. increments of midspan deflection of IG. Load application was discontinued at a deflection of 3 in.

The eighth loading used the same setup as the first. Again, load was increased by load increments until the applied load vs. midspan deflection curves of EGL and EGR became non-linear. Further load was introduced until a deflection of about 2.5 in. was attained for the exterior joist-girders.

The ninth loading repeated the seventh in order to determine the ultimate load capacity of IG. W3R, a web member of EGL, failed due to compression buckling before the ultimate load could be reached for IG.

For the tenth loading, the load points were moved so that IG could be loaded directly. Load was applied until a midspan deflection of more than 7 in. was achieved.

The eleventh and final loading was performed after welds were added to the spacers of the members W3, W5, W5R, and W3R on EGR to help prevent the buckling which occurred on EGL during the ninth loading. The rams and primary load points were repositioned directly over EGR. The secondary load points were put over EGL. Load was applied by load increment and then by deflection increment of EGR until a buckling failure occurred in web member W3R of EGR.

It should be noted that the unbalanced loadings used during the flush framed testing were not performed on the two subsequent specimens. Because of this, an in-depth analysis of those loadings will not be covered at this time.

2.5.3 Stub-Girder Tests

The load configurations for the stub-girder tests are shown in Figure 2.20. For the first loading, the load points were placed at 46.88 in. on either side of the interior joist-girder. The load was increased to reach the nominal service load of 46.9 k at each end reaction of EGL and EGR. The total load reported included self-weight of the joist-

girder, joists, deck and slab, as well as the applied load. Measurements were taken in 5 k increments. The specimen was then unloaded.

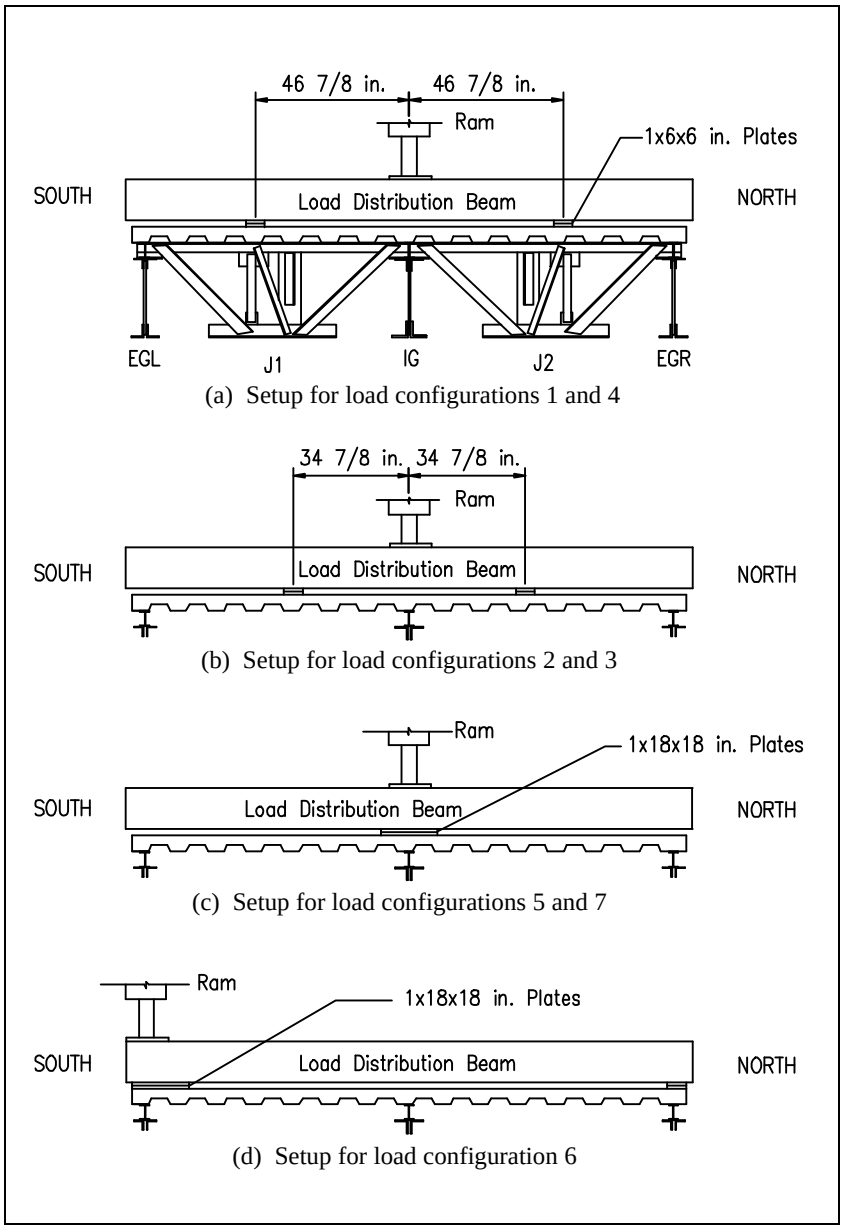

Figure 2.20 Stub-Girder Load Configurations

For the second loading, the load points were placed at 34.88 in. on either side of the interior joist-girder. The load was increased until reaching the nominal service load of 94.6 k at each end reaction of IG. Measurements were taken in 10 k increments, then

reduced to 5 k increments when approaching the service load. The specimen was then unloaded.

The third loading used the same setup as the second. Load was applied until the nominal yield load was attained in IG. Measurements were taken in 20 k increments, then reduced to 10 k and then 5 k increments. Before reaching the nominal yield load, however, the bottom plate of the southwest load point punched into the concrete slab. The floor was unloaded and the 1 in. x 6 in. x 6 in. plates were replaced by 1 in. x 18 in. x 18 in. plates. The floor was then reloaded to near the nominal yield load and subsequently unloaded.

For the fourth loading, the same setup as the first loading was used. Load was to be applied until the nominal yield load was attained in EGL and EGR. Loading was done in 20 k increments of EGL and EGR reactions, then reduced to 10 k and then 5 k increments until the load vs. midspan deflection curve no longer displayed linear elastic behavior. The load was then increased in increments of midspan deflection. Deflection continued to increase with little increase in load. The specimen was unloaded when a load of only approximately 80% of the nominal yield load was reached.

For the fifth loading, the load points were positioned over IG to load it directly in order to determine the ultimate load capacity of the joist-girder. The load was increased until the load vs. midspan deflection curve of IG became non-linear, showing inelastic behavior. Beyond this point, load was applied in increments of the midspan deflection of IG. Loading was terminated when the load vs. deflection curve established a plateau. The specimen was then unloaded.

In the sixth loading, the load points were placed over EGL to load it directly so as to determine an ultimate load capacity. Load was increased until the load vs. midspan deflection became non-linear. After that, the load was applied according to increments of midspan deflection, until a deflection of approximately 4.8 in. was reached. The specimen was then unloaded.

In the seventh and final loading, the load points were moved back over IG to again attempt to determine and ultimate load. The load was increased until the load vs. midspan deflection became non-linear. Beyond this point, loading was done in increments of the midspan deflection of IG. Loading was terminated when the midspan deflection of IG reached approximately 6 in. The specimen was then unloaded.

2.5.4 Haunched Girder Tests

The load configurations for the haunched girder tests are shown in Figure 2.18. For the first loading, the load plates were placed directly over the joists at 57 in. to the left of IG and 60 in. to the right of IG. The load was increased until reaching the nominal service load of 49.6 k at each end reaction of EGL. Measurements were taken in 5 k increments of applied load at each end reaction. The specimen was then unloaded.

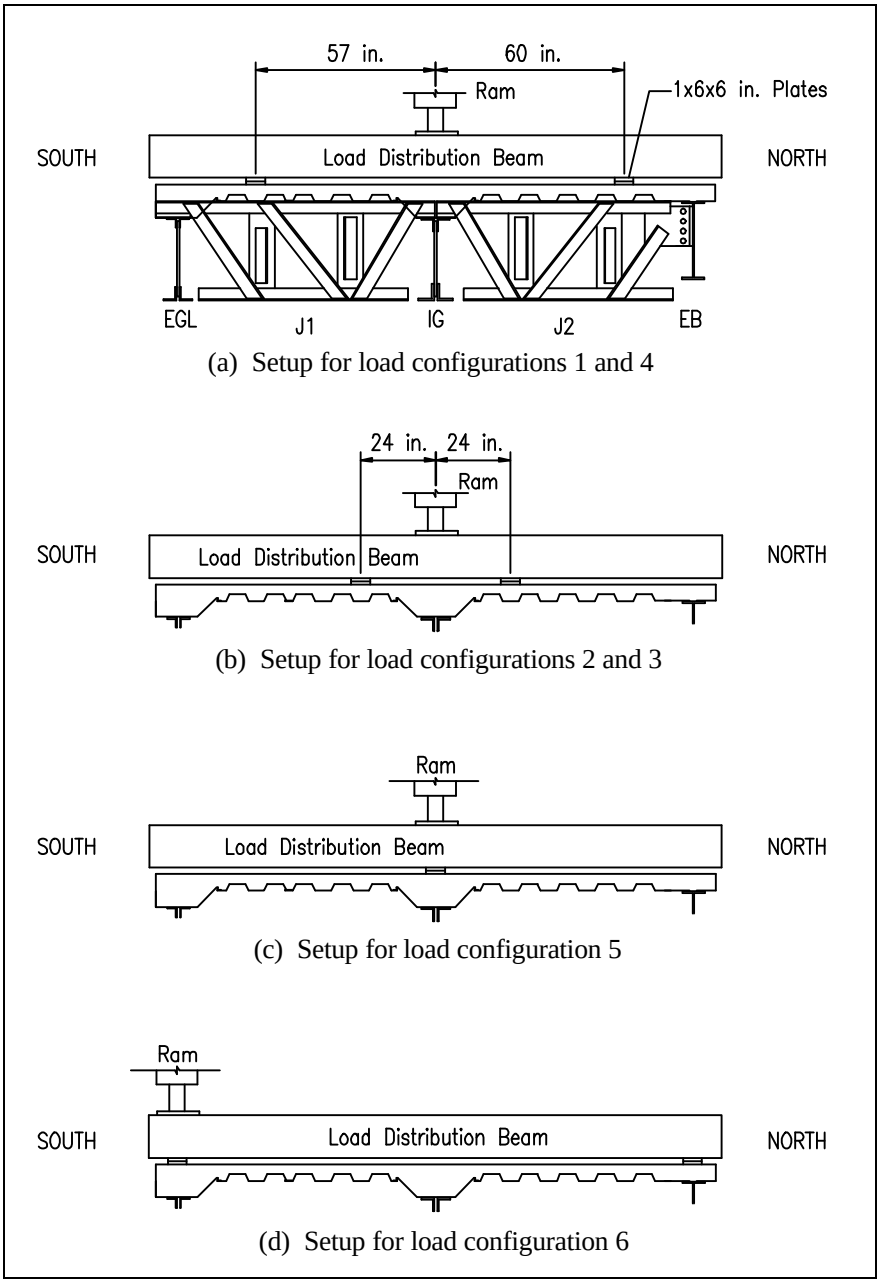

Figure 2.21 Haunched Girder Load Configurations

In the second loading, the load plates were moved to locations that were 24 in. to either side of IG so that it could be loaded principally. The load was increased until reaching the nominal service load of 99.4 k at each end reaction of IG. Measurements

were taken in 20 k increments, then reduced to 10 k increments and then 5 k increments when approaching the service load. The specimen was then unloaded.

The third loading used the same setup as the second. Load was applied until the nominal yield load was attained in IG. Measurements were taken in 20 k increments, then reduced to 10 k and then 5 k increments. The load was increased until a value of 148.4 k at each end reaction was achieved. The specimen was then unloaded.

For the fourth loading, the load plates were moved back to their positions for the first test. Load was to be applied until the nominal load was attained in EGL and/or EB. Loading was done in 30 k increments of EGL and EB reactions, then reduced to 10 k and then 5 k increments until the load vs. midspan deflection curve for EB no longer displayed linear elastic behavior. The load was then increased by increments of deflection of EB until the deflection at midspan had reached 3.1 in. The specimen was then unloaded.

The fifth loading had the load plates moved so that IG would be loaded directly over the top chord. This test was to determine the ultimate load capacity of IG. Load was increased until the load vs. midspan deflection curve of IG became non-linear, showing inelastic behavior. Beyond this point, load was increased by increments of the midspan deflection of IG. Loading was terminated when the deflection reached approximately 4.5 in. The specimen was then unloaded.

For the sixth and final loading, the load plates were placed directly over EGL to load it directly so as to determine an ultimate load capacity. Load was increased until the load vs. midspan deflection curve of EGL became non-linear. After that, the load was applied according to increments of midspan deflection, until a plateau was established in the load vs. deflection curve. Loading was discontinued once a deflection of approximately 4.4 in. was reached at midspan. The specimen was then unloaded.

CHAPTER III
TEST RESULTS

3.1 General

Results of testing on the three floor systems are now presented and discussed. All of the data is reported based on total load values. These represent the complete loadings of each specimen, including dead and applied loads. Dead load refers to the load constituted by the weight of the joists, joist-girders, deck and concrete. The weight of the load distribution beams was not included for two reasons. The changing locations of the load points during the course of testing meant that the distribution of dead weight from the spreader beams varied. Also, the contribution of the load distribution beams to the system dead weight during the flush framed testing was determined to be relatively small.

Applied load refers to the external loading of the structure using the hydraulic rams. Plots of the data display total load versus various measured responses such as strain and vertical deflection. Each plot depicts the response of the specific test specimen through its entire load history, as described in Chapter 2. Summary sheets and plots depicting the data collected for the joist-girders in each setup may be found in Appendix B. Complete sets of data and associated plots may be found in the appendices of the project reports (Kigudde et al 1998, Showalter et al 1999a, Showalter et al 1999b).

All loading data collected have been referenced from a common point. A zero load reading indicates that a specimen was not subjected to any load, including its self-weight. The first data point in each set represents the joist-girder, joist and deck structure self-weight. The second data point is the sum of that self-weight and the weight of the concrete slab. Because the self-weight of the specimen was not measured directly, the first data point was extrapolated based on data obtained during concrete placement. The remaining data points were obtained by adding the value of the second data point to each of the subsequent applied load values.

Several types of loads will be used in the discussion of the test results. Nominal design and yield loads, such as the target loads for the testing cycles noted in Chapter 2, refer to the anticipated total load values needed to reach the design and yield loadings assuming nominal material properties. These nominal values were specified as F_y = 50 ksi for the steel in all three specimens and f_c' = 3.0 ksi for the flush framed and stub girder specimens and f_c' = 4.0 ksi for the haunched girder specimen. Actual service and yield loads refer to the loads based on measured material properties. The experimental total load on a given joist-girder was determined by adding together the load cell readings for each joist-girder end support and then adding the tributary self-weight of the particular specimen. Due to a problem with faulty readings for the west support of the interior joist-girder during the stub-girder tests, total load for that specimen was estimated as double the load cell readings for the east end support plus the tributary self-weight of the specimen.

The results of concrete cylinder tests, to determine the actual strengths of the concrete slabs at testing, are shown in Table 3.1. It should be noted that for the flush framed specimen, the strength was considerably higher than the specified nominal value. The results of steel coupon tests, to determine the actual strengths of the specimen chord members, are shown in Tables 3.2 - 3.4. All concrete compressive cylinder and steel tensile coupon tests were performed at the Virginia Tech Structures and Materials Laboratory.

Table 3.1 Measured Concrete Compressive Strengths

Test Setup	f_c' (psi)
Flush Framed Girder	4 900
Stub Girder	3 000
Haunched Girder	4 500

Table 3.2 Measured Flush Framed Girder Bottom Chord Steel Strengths

Girder	F_y (psi)	Average F_y (psi)	F_u (psi)	Average F_u (psi)
EGL	59 800		82 200	
	60 900		84 000	
	61 200		83 700	
	58 900	60 200	82 900	83 200
IG	54 800		77 200	
	54 700		77 500	
	55 300		78 100	
	55 200	55 000	78 100	77 700
EGR	58 700		80 900	
	60 400		83 500	
	61 800		83 900	
	59 300	60 100	81 700	82 500

Table 3.3 Measured Stub-Girder Bottom Chord Steel Strengths

Girder	F_y (psi)	Average F_y (psi)	F_u (psi)	Average F_u (psi)
EGL	53 800		79 600	
	54 700		80 000	
	55 000		80 900	
	54 800	54 600	80 000	80 100
IG	62 000		83 900	
	61 600		83 200	
	57 600		80 600	
	56 600	59 400	80 200	82 000
EGR	53 800		79 900	
	53 800		79 400	
	53 400		79 600	
	53 100	53 500	79 200	79 500

Table 3.4 Measured Haunched Girder Top and Bottom Chord Steel Strengths

Girder	Member	F_y (psi)	Average F_y (psi)	F_u (psi)	Average F_u (psi)
EGL	Top Chord	57 400		86 100	
	Top Chord	58 700	58 000	86 600	86 400
	Bottom Chord	54 600		82 100	
	Bottom Chord	55 700		81 500	
	Bottom Chord	56 600		82 200	
	Bottom Chord	54 400	55 300	82 600	82 100
IG	Top Chord	56 200		81 900	
	Top Chord	55 200	55 700	82 100	82 000
	Bottom Chord	52 900		83 600	
	Bottom Chord	53 800		83 700	
	Bottom Chord	52 100		83 200	
	Bottom Chord	55 000	53 400	84 300	83 700

3.2 Flush Framed Girder Tests

3.2.1 EGL

The joist-girder design was based on the assumption that bottom chord yielding at midspan would be the controlling limit state. The nominal design load was found to be 93.7 kips and the nominal yield load was 155.9 kips. The expected total load that would cause bottom chord yielding at midspan was 189.5 kips, based on values for steel and concrete strengths from tensile coupon and compressive cylinder test results. The actual design load was found to be 113.9 kips. At this actual design load, the midspan deflection was interpolated from loading 3 results to be 1.28 in.

EGL failed by compression buckling of web member W3R during test 9 with a total load of 160.8 kips, and a vertical deflection at midspan of 2.74 in. At failure, the bottom chord was just beginning to show signs of yielding, as seen in Figure 3.1. The maximum total load on EGL was 174.3 kips (1.12 x nominal yield load, 0.92 x actual yield load) during 8. Total load vs. midspan deflection is shown in Figure 3.2.

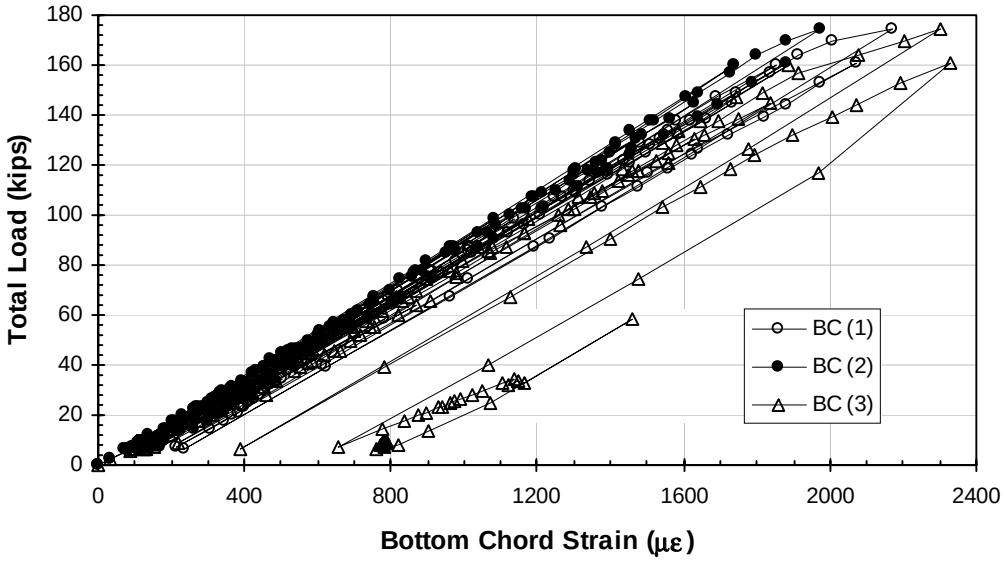

Figure 3.1 Flush Framed Girder EGL Total Load vs. Bottom Chord Strain

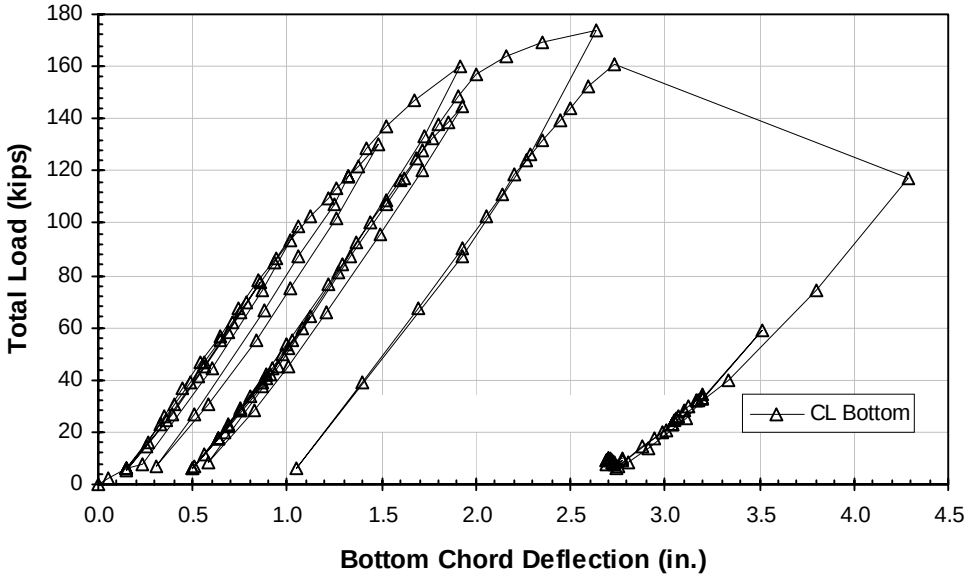

Figure 3.2 Flush Framed Girder EGL Total Load vs. Midspan Deflection

3.2.2 IG

The joist-girder design was based on the assumption that bottom chord yielding at midspan would be the controlling limit state. The nominal design load was found to be 189.1 kips and the nominal yield load was 314.7 kips. The expected total load that would cause bottom chord yielding at midspan was 351.2 kips, based on values for steel and concrete strengths from tensile coupon and compressive cylinder test results. The actual design load was found to be 210.8 kips. For this load, the midspan deflection was interpolated from loading 3 results to be 1.15 in.

The welds on the fillers of web members W3, W3R, W5 and W5R failed at approximately 331 kips during loading 9. Shortly thereafter, the webs began to buckle excessively. Loading 10 was terminated at a total load of about 329 kips with a midspan deflection of about 7.2 in, because no further load was being carried. At termination, the bottom chord showed significant yielding, as shown in Figure 3.3. The maximum total load on IG was 341.4 kips, (1.08 x nominal yield load, 0.97 x actual yield load) reached during loading 9. A plot of total load vs. midspan deflection is shown in Figure 3.4.

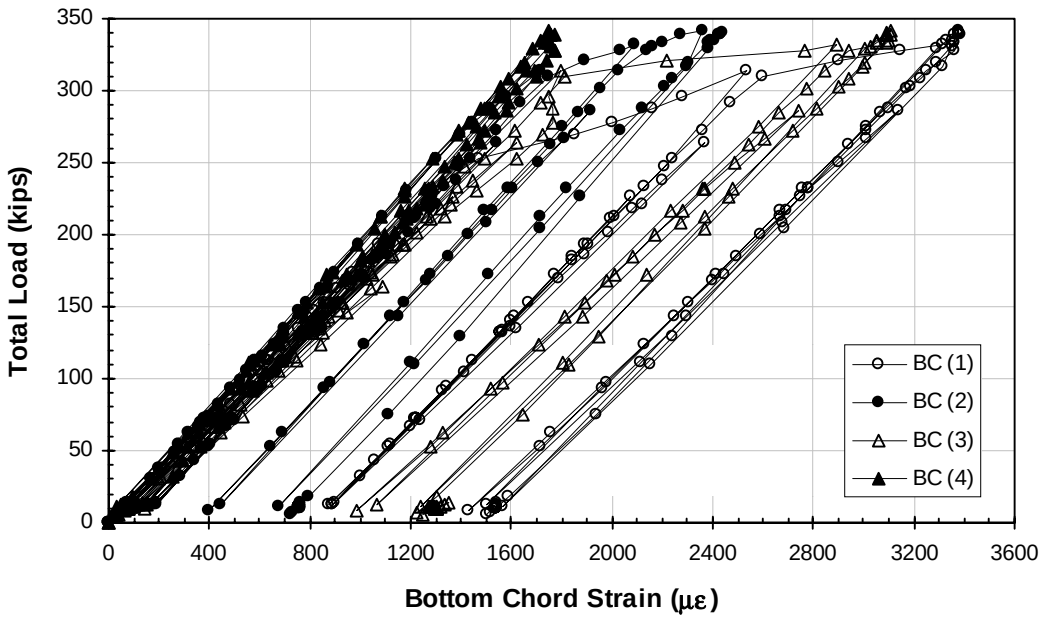

Figure 3.3 Flush Framed Girder IG Total Load vs. Bottom Chord Strain

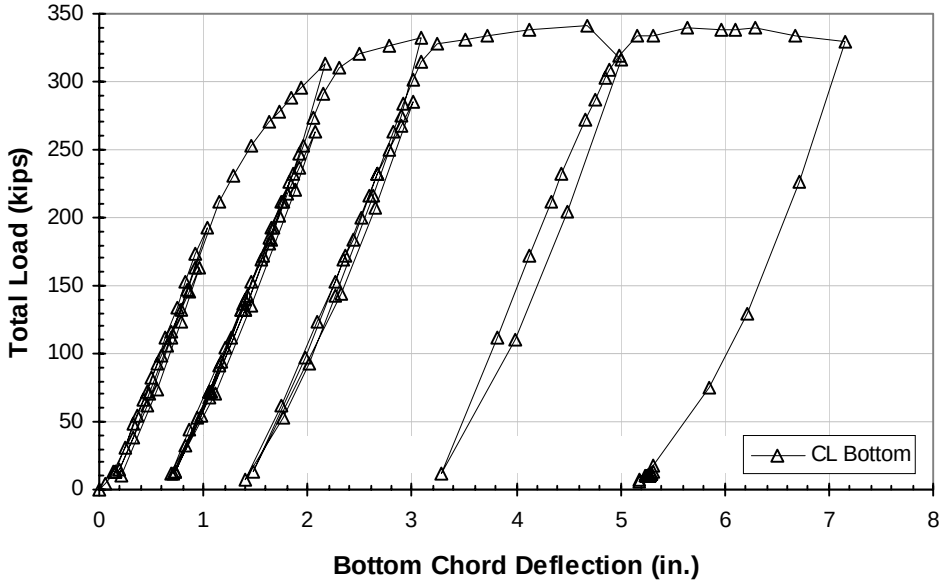

Figure 3.4 Flush Framed Girder IG Total Load vs. Midspan Deflection

3.2.3 EGR

The joist-girder design was based on the assumption that bottom chord yielding at midspan would be the controlling limit state. The nominal design load was found to be 93.7 kips and the nominal yield load was 155.9 kips. The expected total load that would cause bottom chord yielding at midspan was 189.0 kips, based on values for steel and concrete strengths from tensile coupon and compressive cylinder test results. The actual design load was found to be 113.5 kips. At this actual design load, the midspan deflection was interpolated from loading 3 results to be 1.29 in.

EGR failure was due to compression buckling of web member W3R during loading 11 with a total load of 165.9 kips and a vertical deflection at midspan of 3.1 in. At failure, the bottom chord had not begun to yield, as seen in Figure 3.5. The maximum total load carried by EGR was 172.9 kips (1.11 x nominal yield load, 0.91 x actual yield load) during loading 8. A plot of total load vs. midspan deflection is shown in Figure 3.6.

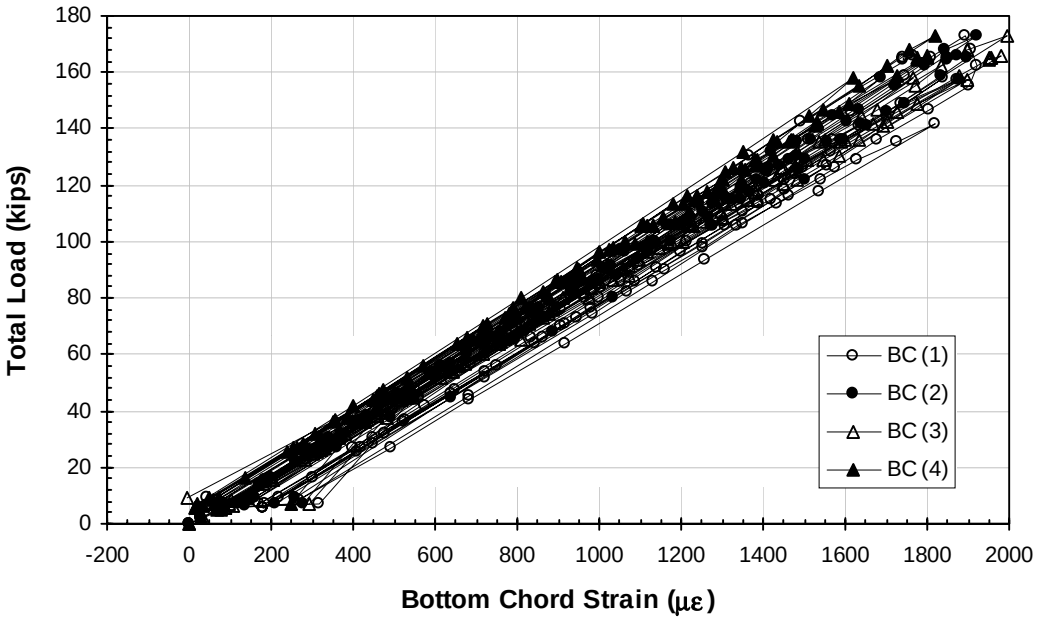

Figure 3.5 Flush Framed Girder EGR Total Load vs. Bottom Chord Strain

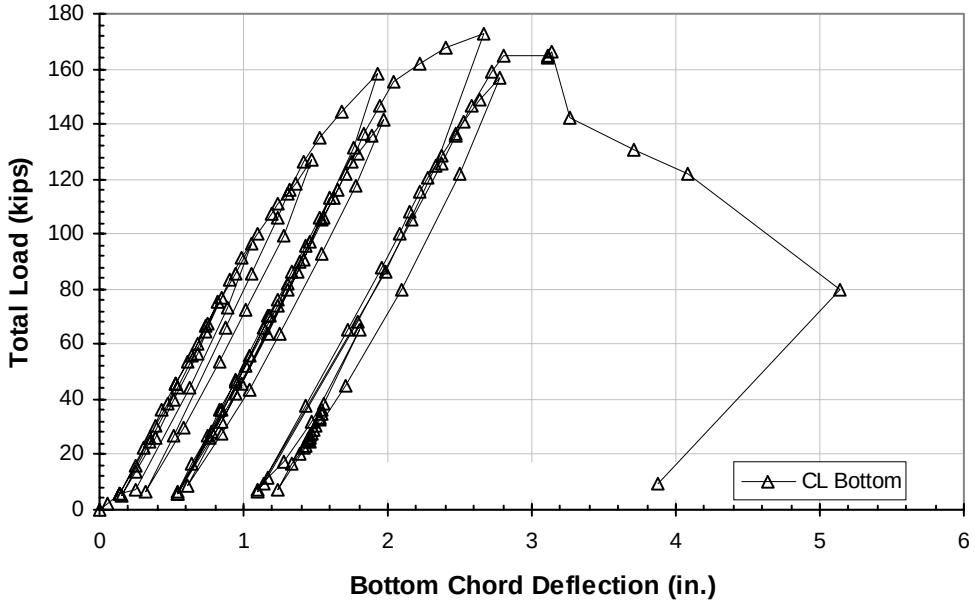

Figure 3.6 Flush Framed Girder EGR Total Load vs. Midspan Deflection

3.3 Stub-Girder Tests

3.3.1 EGL

The joist-girder design was based on the assumption that bottom chord yielding at midspan would be the controlling limit state. The nominal design load was found to be 93.7 kips and the nominal yield load was 155.9 kips. The expected total load that would cause bottom chord yielding at midspan was 169.7 kips, based on measured values for steel yield stress and concrete compressive strength. The actual design load was found to be 102.0 kips. At this actual design load, the midspan deflection was interpolated from loading 3 results to be 1.18 in.

In loading 4, when attempting to achieve the nominal yield load of 155.9 kips for the exterior joist-girders, only a maximum total load of 134.6 kips was reached. This translates to approximately 0.86 x nominal yield load and 0.79 x actual yield load, with a midspan deflection of 1.77 in. In loading 6, when the joist-girder was being loaded directly, a maximum total load of 148.7 kips (0.95 x nominal yield load, 0.88 x actual yield load) was reached, with a corresponding midspan deflection of 3.19 in.

EGL failed as shear connection was lost along the east third span during loading 6 with a total load of 148.7 kips, a vertical deflection at midspan of 3.19 in. and a vertical deflection at the east third point of 3.17 in. Also, a hinge formed at the east third point of the top chord while some yielding occurred in the bottom chord at the same location. At failure, the bottom chord had not yielded significantly at midspan, as seen from a plot of total load vs. bottom chord strain in Figure 3.7. The extent of yielding at the east third point is not known due to a lack of instrumentation at that location. The maximum total load on EGL was 148.7 kips. A plot of total load vs. midspan deflection is shown in Figure 3.8.

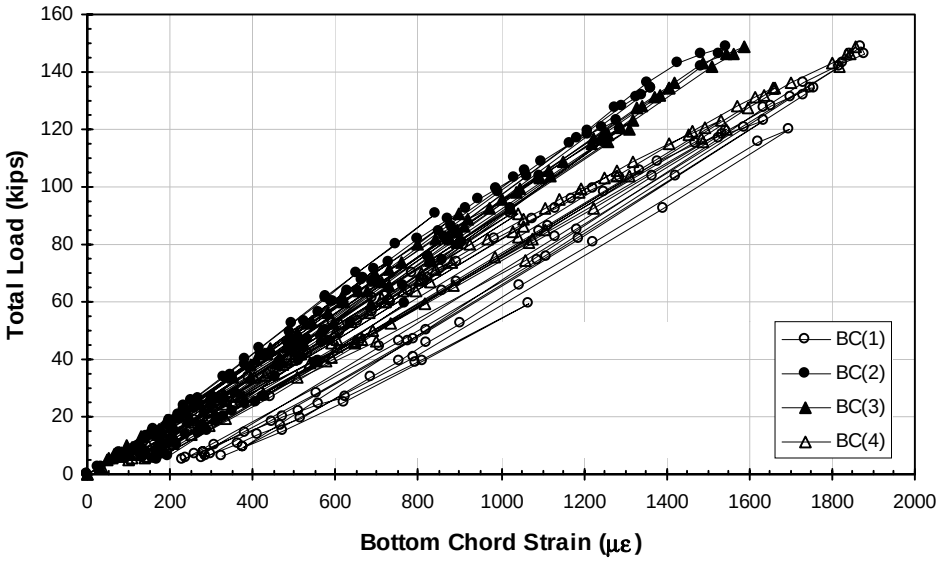

Figure 3.7 Stub-Girder EGL Total Load vs. Bottom Chord Strain

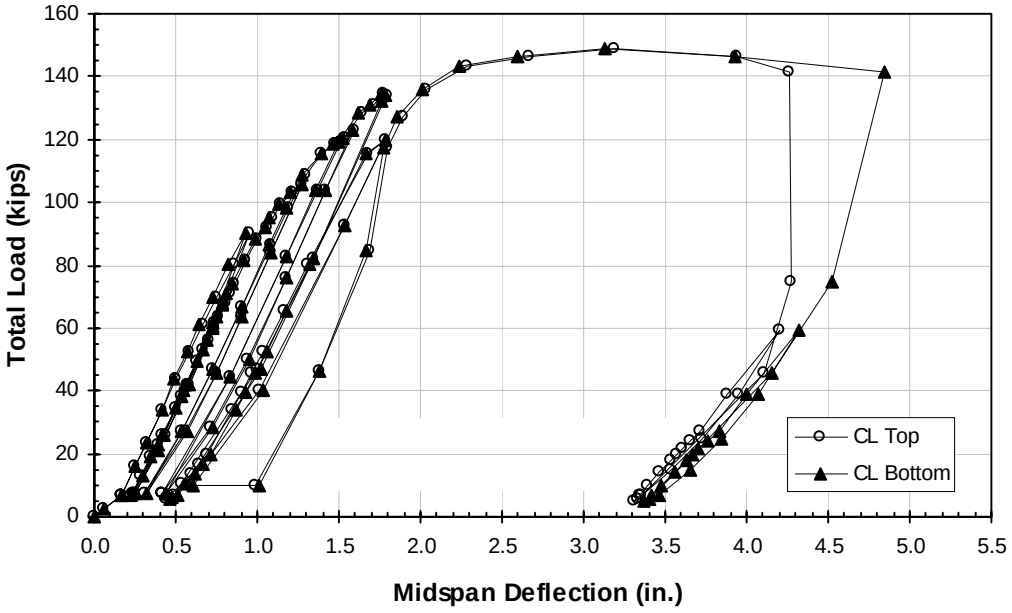

Figure 3.8 Stub-Girder EGL Total Load vs. Midspan Deflection

3.3.2 IG

The joist-girder design was based on the assumption that bottom chord yielding at midspan would be the controlling limit state. The nominal design load was found to be 189.1 kips and the nominal yield load was 314.7 kips. The expected total load that would cause bottom chord yielding at midspan was 370.6 kips, based on measured values for steel yield stress and concrete compressive strength. The actual design load was found to be 222.7 kips. For this load, the midspan deflection was interpolated from loading 3 results to be 1.35 in.

During loading 3, the plates at the southwest load point began punching into the deck. As a result, loading was discontinued. Once larger plates were put in position, the floor was reloaded to a maximum load of 298.2 kips (0.95 x nominal yield load, 0.80 x actual yield load) when trying to reach the nominal yield load. The corresponding TC midspan deflection was found to be 2.96 in.

When applying load directly to failure in loading 5, loading was terminated at a total load of approximately 299.0 kips, with a TC midspan deflection of about 3.87 in. At this point, the larger plates were crushing into the slab due to its excessive deformation. At termination of loading, the bottom chord had not yielded significantly, as seen in Figure 3.9. The maximum total load on IG was 299.0 kips (0.95 x nominal yield load, 0.81 x actual yield load during loading 5. The girder was reloaded in loading 7, but no greater capacity could be achieved. A plot of total load vs. midspan deflection is shown in Figure 3.10.

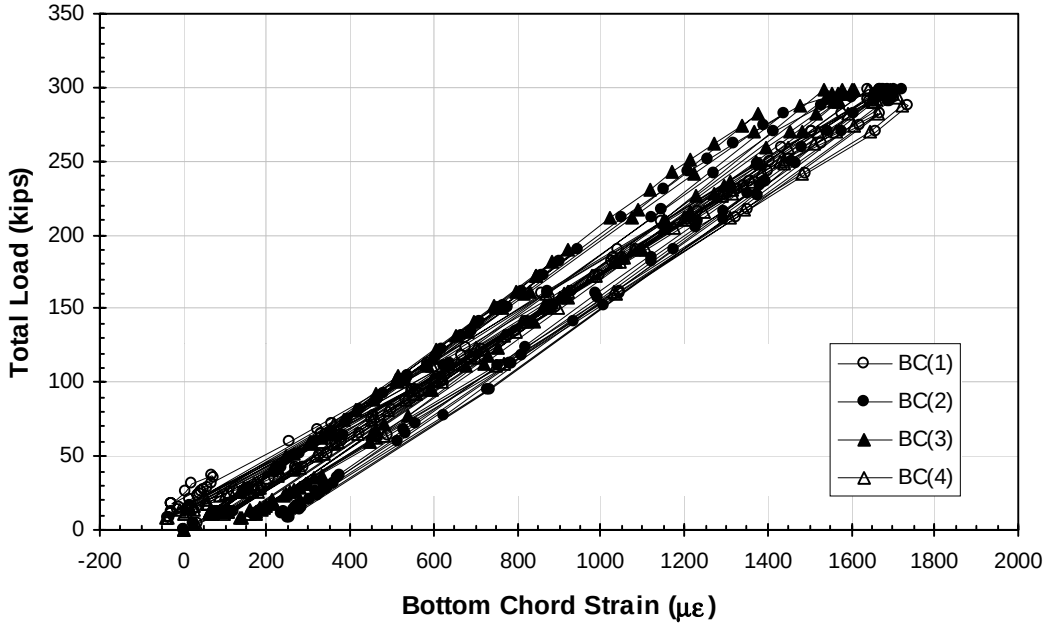

Figure 3.9 Stub-Girder IG Total Load vs. Bottom Chord Strain

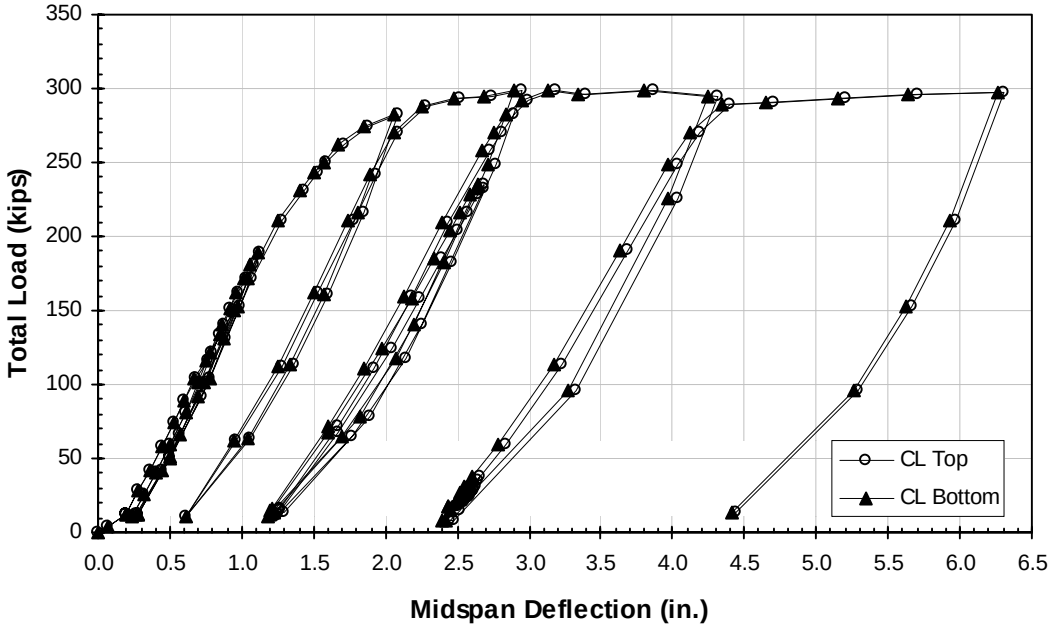

Figure 3.10 Stub-Girder IG Total Load vs. Midspan Deflection

3.3.3 EGR

The joist-girder design was based on the assumption that bottom chord yielding at midspan would be the controlling limit state. The nominal design load was found to be 93.7 kips and the nominal yield load was 155.9 kips. The expected total load that would cause bottom chord yielding at midspan was 166.4 kips, based on measured values for steel yield stress and concrete compressive strength. The actual design load was found to be 100.0 kips. At this actual design load, the midspan deflection was interpolated from loading 3 results to be 1.19 in. The maximum load achieved on EGR was 141.3 kips (0.91 x nominal yield load, 0.85 x actual yield load) and the midspan deflection was interpolated from loading 4 results to be 2.62 in. The joist-girder was not directly loaded to failure because of loss of shear connection along the west third span during loading 3.

EGR failed due to loss of shear connection, and thus loss of composite action of the west third span during loading 3. As IG was being loaded, the deflection at the longitudinal centerline of the slab caused a rotation of the slab edge over EGR. This created tensile stresses in the slab in the transverse direction. The concrete split in a series of longitudinal cracks directly along the stud line on the west third of the span. At failure, the bottom chord had not yielded significantly at midspan, as seen from Figure 3.11. The maximum total load on EGR was 141.3 kips during loading 4. A plot of total load vs. midspan deflection is shown in Figure 3.12.

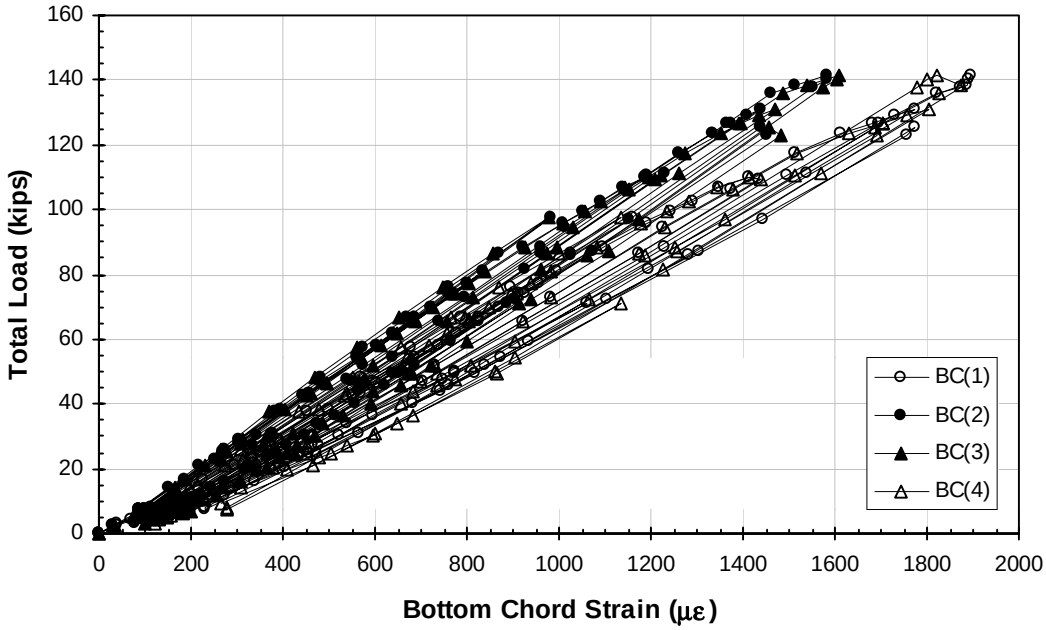

Figure 3.11 Stub-Girder EGR Total Load vs. Bottom Chord Strain

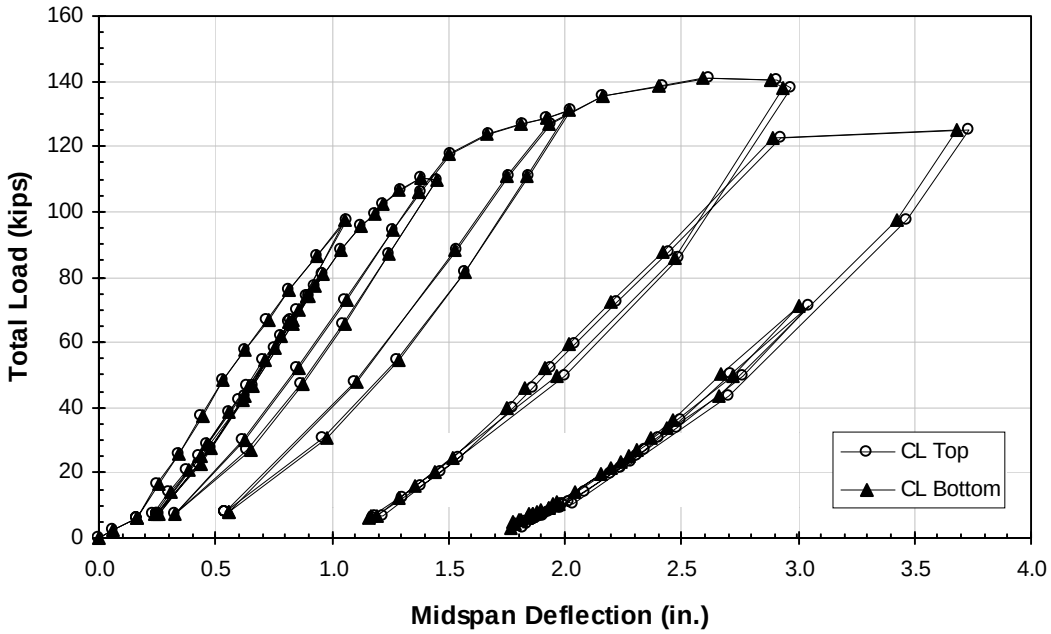

Figure 3.12 Stub-Girder EGR Total Load vs. Midspan Deflection

3.4 Haunched Girder Tests

3.4.1 EGL

The joist-girder was designed assuming that bottom chord yielding at midspan would control but a significant contribution (25% of tensile strength) to capacity would also be made by the top chord carrying tensile forces as well. The nominal design load was found to be 99.1 kips and the nominal yield load was 164.1 kips. The actual total load was 181.7 kips, based on measured values for steel yield stress and concrete compressive strength. The actual design load was found to be 109.7 kips. At this load, the midspan deflection was interpolated from loading 4 results to be 1.05 in.

In loading 4, when attempting to reach the nominal yield load, only 147.0 kips was achieved (0.90 x nominal yield load, 0.81 x actual yield load) due to yielding in EB. At this load, the midspan deflection measured 1.48 in. In loading 6, when the girder was being loaded directly, a maximum load of 176.6 kips (1.08 x nominal yield load, 0.97 x actual yield load) was reached. The corresponding midspan deflection was approximately 3.36 in.

EGL failed as a result of yielding of the bottom chord during loading 6. The yielding began at the east third point at a total load of 163.0 kips (as can be seen in Figure 3.13) with a corresponding vertical deflection at midspan of 1.97 in. and a vertical deflection at the east third point of 1.84 in. From this point, an additional 13 kips

increased the load to its maximum value. Load was applied until a midspan deflection of over 4 in. was achieved. A distinct yield plateau can be seen in Figure 3.14. In addition, yielding was beginning to occur at midspan and at the west third point of the bottom chord.

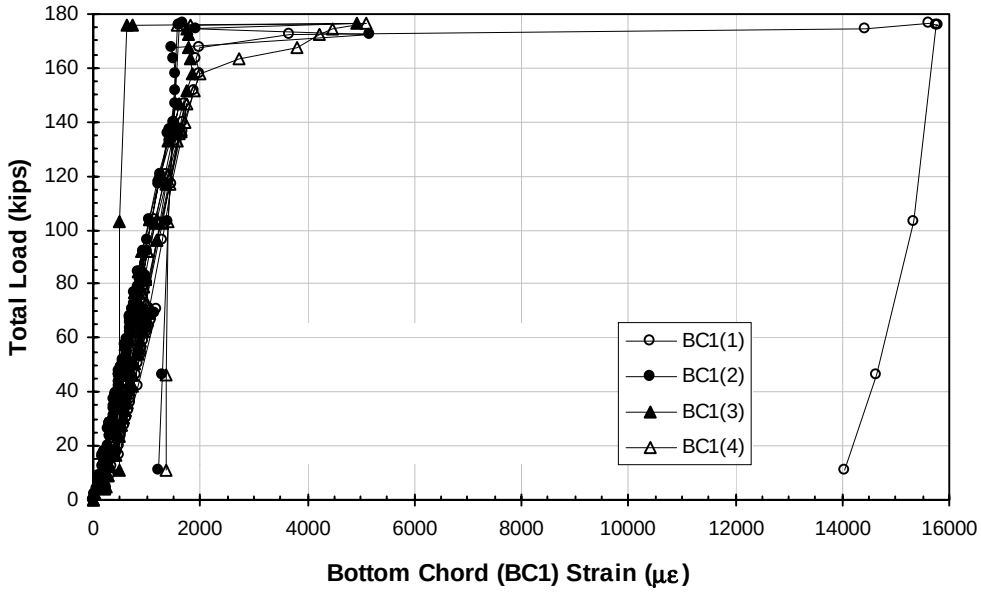

Figure 3.13 Haunched Girder EGL Total Load vs. Bottom Chord (1) Strain

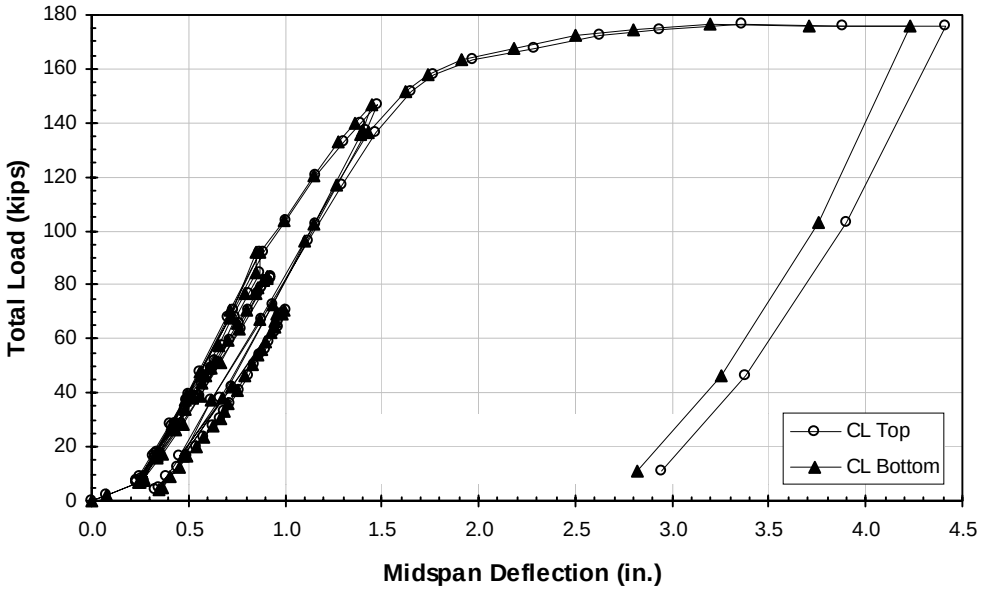

Figure 3.14 Haunched Girder EGL Total Load vs. Midspan Deflection

3.4.2 IG

The joist-girder was designed assuming that bottom chord yielding at midspan would control but a significant contribution (25% of tensile strength) to capacity would also be made by the top chord carrying tensile forces as well. The nominal design load was found to be 198.8 kips and the nominal yield load was 329.8 kips. The actual total load was 353.2 kips, based on measured values for steel yield stress and concrete compressive strength. The actual design load was found to be 212.8 kips. At this load, the TC midspan deflection was interpolated from loading 3 results to be 1.25 in.

During loading 3, when attempting to reach the nominal yield load, a total load of 296.8 kips (0.90 x nominal yield load, 0.84 x actual yield load) was achieved. For this load, a midspan deflection of 1.70 in. was measured for the TC. The girder was loaded to a maximum total load of 409.1 kips (1.24 x nominal yield load, 1.16 x actual yield load) during loading 5 when the girder was being loaded directly. The corresponding TC midspan deflection was approximately 4.60 in.

Failure of IG was a result of yielding of the bottom chord during loading 5. Yielding was fully occurring at the east third point at a total load of 404.4 kips with a corresponding midspan vertical deflection of 4.45 and east third point deflection of 4.11 in. From an examination of total load vs. midspan deflection (Figure 3.15), IG appeared to be yielding at a load of 334 kips. A yield plateau began to develop, yet the average strain was not increasing (Figure 3.16) until a load of 388 kips was reached, at which point several strains began increasing rapidly.

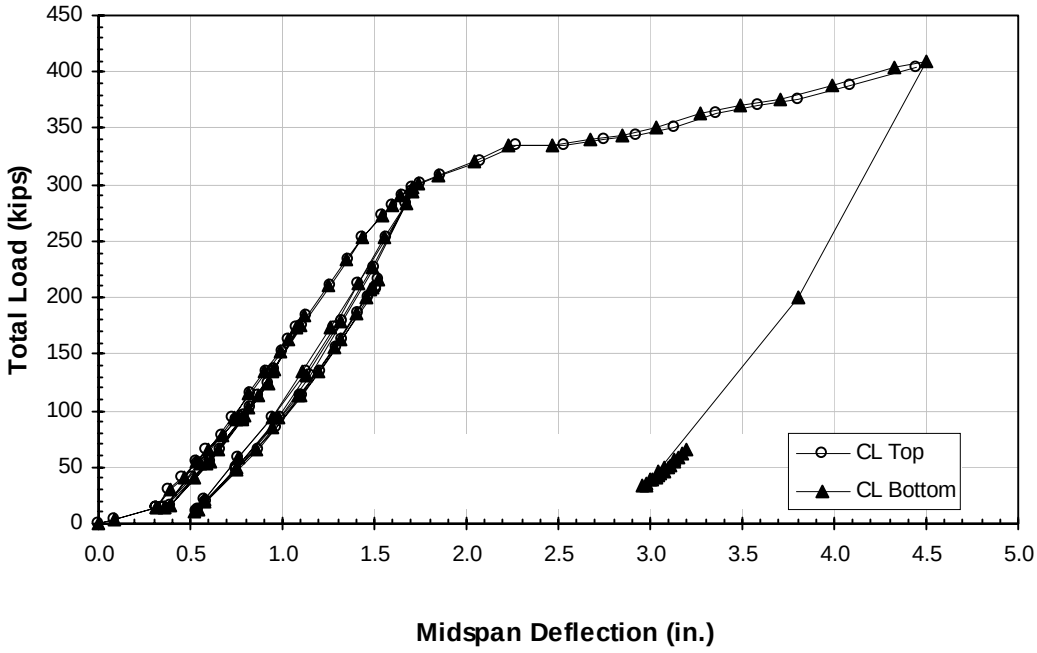

Figure 3.15 Haunched Girder IG Total Load vs. Midspan Deflection

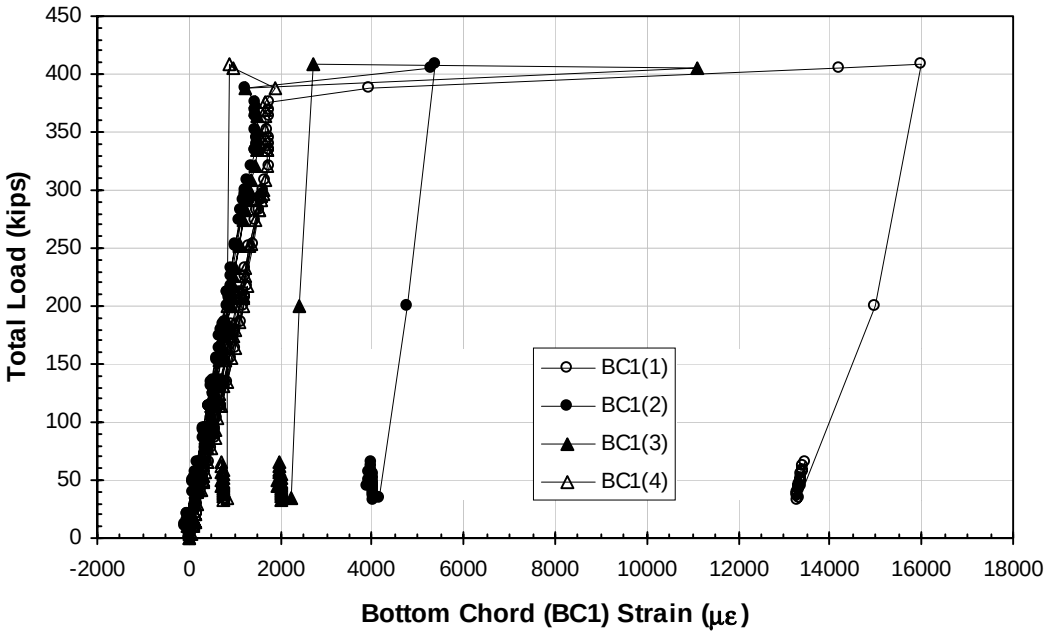

Figure 3.16 Haunched Girder IG Total Load vs. Bottom Chord (1) Strain

CHAPTER IV
ANALYSIS AND INTERPRETATIONS

4.1 General

The purpose of this research was to evaluate whether the three proposed configurations were efficient means of generating composite action in joist-girders. The research was also performed to examine the effectiveness of using the model for standard composite open-web joist design (*Proposed* 1996) and determine whether this model could be used for joist-girders in a system where both the joists and joist-girders were designed to act compositely. The joist-girders in each specimen were modeled as standard composite open-web joists as described in the proposed design specification. The controlling limit state in this model was yielding of the bottom chord. This specification came about, in part, from the research previously described in Chapter 1.

The analysis of each specimen began with the determination of the theoretical moment capacities of the joist-girders to be used. These theoretical capacities were determined by the yield stresses of the joist-girder bottom chords. From the calculated theoretical moments, the load capacities could then be determined. The testing procedures were then structured to experimentally determine these capacities.

The expected loads, stiffnesses and deflections calculated during the design process will be discussed and compared to the actual values that were measured during testing. Several other issues that were formulated during design or that arose during testing will also be discussed briefly. These issues include the use of differing numbers of bolts in the joist to joist-girder connections of the flush framed setup, and the use of welded rods to stabilize the bottom chords where the joists tied into the joist-girders. A problem that arose during testing of the stub-girder specimen was localized buckling of the joist-girder top chords underneath the joist seats. Finally, the amount of transverse reinforcement was varied among the specimens to evaluate its impact on the joist-girder capacities. This appeared especially significant for exterior joist-girders where a free edge existed.

4.2 Analytical Modeling

Nucor Research and Development began the design of each specimen with the assumption that yielding of the bottom chord would be the controlling limit state according to the proposed design methodology (*Proposed* 1996). Thus, the design of the specimens began with the determination of the theoretical moment capacity of each joist-girder. The moment arm is defined as the distance from the centroid of the bottom chord to the center of compressive resistance in the concrete. This generalization, which ignores

any contribution by the top chord, is made because the centroid of the top chord is very close to the neutral axis of the composite system and has been found not to contribute significantly to the moment capacity. This concept has been confirmed by a number of researchers, including Azmi (1972), Curry (1988), and Lauer et al. (1996). In all cases, it is assumed that the slab and joist-girder act as a fully composite system with adequate shear connection.

The theoretical capacities of the joist-girders in the flush framed and stub-girder test specimens were determined according to the loads which would cause full yielding of the bottom chord at midspan. The maximum tensile force to be carried in the bottom chord, T, equals the value of A_sF_y for that chord. This design philosophy assumes the concept of the "balanced" design case. This means that the amount of shear connection provided for the composite girder, ΣQ, is equal to the bottom chord yield force, T. The balanced condition also assumes that essentially no force acts in the top chord because of the proximity of the top chord to the line of action of the shear connectors. The balanced condition means that there is sufficient shear connection to fully develop yielding in the bottom chord, but not so much as to be clearly over-connected.

For the haunched girder specimen, the model was revised to include a tensile force contribution by the joist-girder top chord. For this specimen, the top chord was considered to carry a significant amount of tensile load and would therefore contribute to the overall girder moment capacity due to the increased concrete cross-sectional area in compression. As a result, the theoretical capacity of each joist-girder was a combination of full yielding in the bottom chord and a percentage, in this case 25%, of full yielding in the top chord.

For each specimen, predicted moments were first calculated for the nominal material properties based on the design philosophy outlined previously. The moments were predicted for nominal values at design and yield loads respectively. Material testing was also performed in the laboratory prior to joist-girder testing to measure the actual material properties of the bottom chord members of each joist-girder. Design and yield moments were calculated based on these actual material properties. These moments were then used to predict the actual design and yield loads expected for each joist-girder.

4.3 Load Capacity

The load capacity of each joist-girder was identified as the total load that could be applied to the system. This total load was made up of three components: the distributed dead load of the joist-girder (self-weight), the concentrated dead load of the joists and slab, and the concentrated applied "live" load. The dead load was determined by combining the theoretical weight of the joist-girders, joists, steel deck and the actual weight of the concrete slab that was measured at placement. The applied load component was simply the amount of applied load measured directly on each joist-girder during testing.

4.3.1 Predicted Loads

Once moment capacities had been calculated, the loads required to achieve those moments were determined through a static analysis of each joist-girder. This load calculation process began with the development of an equilibrium equation using the assumed design values of w_g and R_{sj} and the calculated values for M_{dn}, M_{yn}, M_{dm}, and M_{ym}.

$$M = 15R_L - 5R_{sj} - 15(15/2)w_g - 5P \qquad \text{[Eq. 4-1]}$$

$$R_L = R_{sj} + 15w_g + P \qquad \text{[Eq. 4-2]}$$

where: M = moment at centerline of joist-girder (kip-ft)

M_{dn} = predicted design moment (nominal material properties)

M_{yn} = predicted yield moment (nominal material properties)

M_{dm} = predicted design moment (measured material properties)

M_{ym} = predicted yield moment (measured material properties)

P = load applied by each hydraulic ram (kips)

R_L = reaction at end of joist-girder (kips)

R_{sj} = self-weight of concrete slab, metal deck, and joist (kips)

w_g = self-weight of joist-girder (kips/ft)

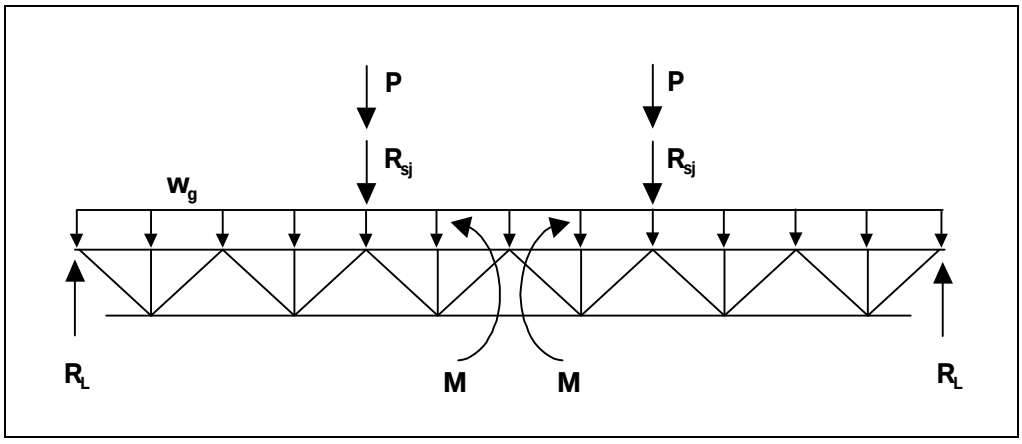

Figure 4.1 Force Diagram Representing Joist-Girder Loading

From Equation 4-1, the particular applied load *P* being sought was determined. This load was then doubled (because there were two load points) and added to the complete dead load to generate the total load, *TL*, on each joist-girder. This is represented as:

$$TL = 2R_L = 2(P + R_{sj} + 15w_g) \qquad \text{[Eq. 4-3]}$$

4.3.2 Experimental Loads

The experimental loads were measured during the course of testing. These loads combined the total dead load of each specimen and the applied load introduced by the hydraulic rams on each joist-girder. It can be seen from Table 4.1 that the predicted loads based on the nominal material properties were conservative for the flush framed girder specimen and the haunched girder specimen, but not for the stub girder specimen. When measured material properties were considered, only the haunched girder specimen, particularly the interior girder, remained conservative, although the interior girder total load came within 3% of the anticipated value for the flush framed specimen.

Table 4.1 Comparison of Experimental to Predicted Load Capacities

Specimen / Girder		TL_{dn} (kips)	TL_{yn} (kips)	TL_{dm} (kips)	TL_{ym} (kips)	TL_e (kips)	TL_e/TL_{yn}	TL_e/TL_{ym}
Flush Framed	EGL	93.7	155.9	113.9	189.5	174.3	1.12	0.92
	IG	189.1	314.7	210.8	350.9	341.4	1.08	0.97
	EGR	93.7	155.9	113.5	189.0	172.9	1.11	0.91
Stub	EGL	93.7	155.9	102.0	169.7	148.7	0.95	0.88
	IG	189.1	314.7	222.7	370.6	299.0	0.95	0.81
	EGR	93.7	155.9	100.0	166.4	141.3	0.91	0.85
Haunched	EGL	99.1	164.1	109.7	181.7	176.6	1.08	0.97
	IG	198.8	329.8	212.8	353.2	409.1	1.24	1.16

TL_{dn} = total design load (nominal material properties)
TL_{yn} = total yield load (nominal material properties)
TL_{dm} = total design load (measured material properties)
TL_{ym} = total yield load (measured material properties)
TL_e = maximum total load measured experimentally

4.4 Stiffness

An important aspect of design is the determination of the stiffness of a system, which can be evaluated in terms of the moment of inertia. The moment of inertia, *I*, of a system plays an important role in the determination of deflections and vibration characteristics. The proposed design specification (*Proposed* 1996) states that the effective moment of inertia can be determined by considering only the bottom chord and the transformed section of the slab when evaluating short term deflection checks.

Also, to account for flexibility often found in open-web joists, the deflections based on these effective *I* values should be increased by 15%. For the specimens tested, theoretical composite moments of inertia for all joist-girders were calculated according to methods employed by Nucor Research and Development, as discussed in Section 4.4.1. These calculations were prepared by David Samuelson of Nucor Research and Development and verified by the researchers.

4.4.1 Predicted I_{calc}

The predicted moments of inertia were computed by a methodology currently used by Nucor Research and Development. This method was developed as part of a process to estimate the midspan deflection of a composite joist. First, the non-composite moment of inertia, I_{nc}, and the transformed moment of inertia, I_t, were calculated. The final calculated moment of inertia, I_{calc}, was then found as:

$$I_{calc} = I_t \times \frac{1}{1+C_{slip}} \times \frac{1}{WEF} \times \frac{1}{\Delta_{adj}} \qquad \text{[Eq. 4-4]}$$

where: I_t = transformed moment of inertia,

C_{slip} = coefficient for shear stud slip influences = 0.05

WEF = "Web Effects Factor"

= $\Delta_{Vmax}/\Delta_{wwe}$ where:

Δ_{Vmax} = maximum deflection of total load case found using a stiffness analysis program developed by Nucor accounting for web shortening.

$$\Delta_{wwe} = \frac{5w_g l^4}{384EI_{nc}} + \frac{Px}{24EI_{nc}}\left(3l^2 - 4x^2\right)$$

Δ_{adj} = span/depth adjustment factor developed by Nucor:

$$= 0.91775 + \frac{76.1692}{(span/depth)^2}$$

An example of the complete calculation process can be found in Appendix A.

4.4.2 Experimental I_{exp}

Load and deflection data from the first load cycle on each specimen were considered when determining the composite moments of inertia for the exterior girders. Similarly, data from the second load cycle on each specimen were considered when assessing the composite moments of inertia for the interior girders. To isolate the composite behavior, applied loads and their resulting deflections were used instead of total loads. A series of I_{exp} values were back calculated through the beam deflection equation for two evenly spaced, symmetric loads.

This equation has the form:

$$\Delta_{max} = \frac{Px}{24EI}\left(3l^2 - 4x^2\right) \qquad \text{[Eq. 4-5]}$$

where: Δ_{max} is measured at midspan

P = one of two equal, concentrated loads

x = spacing of load from the girder end

E = modulus of elasticity of steel

I = moment of inertia

l = girder span length

For all specimens, E was assumed to be 29,000 ksi, x = 10 ft, and l = 30 ft. By substituting these values, the equation became:

$$\Delta_{max} = 57.103\left(\frac{P}{I}\right) \qquad \text{[Eq. 4-6]}$$

Rearranging, the equation became:

$$I = 57.103\left(\frac{P}{\Delta_{max}}\right) \qquad \text{[Eq. 4-7]}$$

Using this equation, applied load and deflection data were substituted for P and Δ_{max} to produce a value for I. The moments of inertia were calculated at a series of load increments and then averaged to determine an overall value for each specimen.

As can be seen from Table 4.2, all but two of the joist-girders had higher experimental stiffnesses than predicted. For all three specimens, the interior girders also showed lower stiffnesses than the exterior girders. The haunched specimen had the stiffest joist-girders among the three specimens, followed by the flush framed girders and then the stub-girders.

Table 4.2 Comparison of Experimental to Predicted Moments of Inertia

Setup / Girder		I_{exp} (in.^{4})	I_{calc} (in.^{4})	I_{exp}/ I_{calc}
Flush Framed	EGL	2965	2705	1.10
	IG	5541	5324	1.04
	EGR	2944	2705	1.09
Stub	EGL	3096	3077	1.01
	IG	5709	5930	0.96
	EGR	3137	3077	1.01
Haunched	EGL	3694	3323	1.11
	IG	6152	6400	0.96

I_{exp} = moment of inertia determined from experimental data for load vs. deflection
I_{calc} = moment of inertia provided by Nucor (measured concrete properties)

4.5 Deflections

As noted previously, deflection is tied directly to the stiffness of the system. Generally, the deflection is to be minimized whenever possible. Deflection is important because it is one significant measure of the serviceability of a system.

4.5.1 Predicted Deflections

Historically, deflections were calculated from I_t values that were determined for an approximate or equivalent section of steel and concrete. The deflections were then modified by a factor to consider shear deformation, web flexibility, slip, etc. For these tests, however, the adjustments were made in the calculation of the stiffnesses, I_{calc}. The predicted total deflections were composed of three parts.

First, the deflection due to the distributed dead load of each joist-girder was determined using the elastic deflection equation:

$$\Delta = \frac{5 w_g l^4}{384 E I_{nc}} \qquad \text{[Eq. 4-8]}$$

where w_g, l, E were defined previously and I_{nc} is the joist-girder non-composite moment of inertia.

The second component of joist-girder total deflection was the portion caused by the concentrated dead load of the slab and joists that was transferred to the joist-girder. This was found by the equation:

$$\Delta = \frac{Px}{24 E I_{nc}} \left(3l^2 - 4x^2\right) \qquad \text{[Eq. 4-9]}$$

where P, x, l, E, and I_{nc} were defined previously. As shown in the discussion on stiffness, this equation can be simplified to:

$$\Delta = 57.103 \left(\frac{P}{I_{nc}} \right) \qquad \text{[Eq. 4-10]}$$

The third portion of total joist-girder deflection resulted from the external load applied to the specimen. This portion affected the joist-girders in the form of concentrated loads at the third points and so used the equation, $\Delta = 57.103 \left(\frac{P}{I_{calc}} \right)$, noted earlier. In this case, the load P is now the applied live load and I_{calc} is the calculated composite moment of inertia of the joist-girder including the proper adjustment factors.

4.5.2 Experimental Deflections

The experimental deflections were measured during testing. Table 4.3 summarizes the comparison of the predicted deflection at design load versus the value actually measured during testing. As can be seen, the ability to predict deflection varied significantly with the different setups used, as well as with individual joist-girders within each specimen. This would imply that one standard method is not suitable for determination of deflections in all types of floor system designs.

Table 4.3 Comparison of Experimental to Predicted Deflections at Design Loads

Specimen / Girder		Design Load	Δ_{calc} (in)	Δ_{exp} (in)	$\Delta_{exp}/\Delta_{calc}$
Flush Framed	EGL	113.9	1.24	1.28	1.03
	IG	210.8	1.17	1.15	0.98
	EGR	113.5	1.24	1.29	1.04
Stub	EGL	102.0	1.04	1.18	1.13
	IG	222.7	1.17	1.35	1.15
	EGR	100.0	1.02	1.19	1.17
Haunched	EGL	109.7	1.09	1.05	0.96
	IG	212.8	1.07	1.25	1.17

Δ_{calc} = deflection at design load (measured material properties)
Δ_{exp} = deflection at design load measured experimentally

4.6 Other Issues

4.6.1 Flush Framed Connection Design

The flush framed specimen was designed utilizing different numbers of bolts (Figure 2.5) in the connection details to observe the potential influence that might exist. Three-bolt connections were designed for IG to act as rigid connections. For EGL, three-bolt connections were designed to work in conjunction with the bottom chord braces to act rigidly. Finally, EGR used four-bolt connections that were designed to be flexible. No distinguishing influence was noted between the various connection types used.

4.6.2 Bottom Chord Brace Design

For the flush framed specimen, the connection design between the joists and exterior joist-girders led to the possibility that eccentric loading could cause the exterior joist-girders to displace outward. To study the possible significance of this effect, steel rods were welded to the joists' (J1) bottom chords and to the bottom chord of EGL during testing. EGR was left free so as to provide a basis for comparison. At the design load for the vertical web member, the anticipated tensile load in the brace was expected to be 6.33 kips based on rods having a nominal yield stress of 50 ksi. The measured brace forces are summarized in Table 4.4.

The lateral deflections of the bottom chords were also considered. Measurements were made at midspan of IG and at the third points of the exterior girders. Table 4.5 summarizes the bottom chord lateral deflections at nominal design and yield loads. Positive values for the exterior joist-girders indicate that the bottom chords deflected away from IG. Positive values for IG indicate that the bottom chord moved toward EGL.

Table 4.4 Measured Bottom Chord Brace Forces

	Brace Force (kips) at Nominal Design Load		Brace Force (kips) at Nominal Yield Load	
	East	West	East	West
EGL	3.65	3.54	6.84	7.62

Table 4.5 Maximum Measured Bottom Chord Lateral Deflections

	Nominal Design Values			Nominal Yield Values		
	Load (kips)	East (in.)	West (in.)	Load (kips)	East (in.)	West (in.)
EGL	93.7	0.13	0.12	154.4	0.12	0.19
IG	189.1	0.19	N/A	311.6	0.10	N/A
EGR	93.7	0.06	0.06	154.4	0.10	0.15

4.6.3 Local Buckling of Girder Top Chord at Joist Load Point

The maximum total loads achieved on the joist-girders in the stub-girder specimen were well below what was expected - from 15% to 19% below the expected values. During testing, it was observed that local buckling occurred in the top chords at the joist bearing locations. A possible significant contribution to this reduced carrying capacity may have been that the joist seats attached to the top chords caused local buckling of the chords as the joists rotated during loading of the interior joist-girder.

A minimal amount of research has been reported regarding the influence of a joist bearing on a joist-girder outstanding leg. One report in particular (Galambos 1983) described the investigation of the strength of the outstanding leg of the compression chord of a joist-girder subjected to eccentric forces from joist seats bearing at the panel points.

The report noted, “Simple elastic limit analysis, modeling the outstanding angle leg as a cantilever, indicated that the flange alone, without local reinforcement, could not carry the joist reactions.” Observations of numerous tests, however, showed that failure rarely, if ever, occurred due to joist reactions. A series of fifteen tests were performed to gather data for an analysis. The researchers hoped to develop a formula for the prediction of the ultimate strength of an outstanding angle leg. Additionally, parametric studies were reviewed from which it was concluded that for usual joist end reactions and joist-girder configurations, a formal design check was not required.

It was found that the joist seat reaction would generate a plastic plate mechanism in the outstanding leg. When this deformation continued, a tension field developed. This provided additional inelastic strength that was thought to significantly increase the load capacities of the joist-girder chords beyond what they were expected to support.

A limitation of the tests was that rollers applied the loads directly over the outstanding legs. This meant that the effects of the load were restricted to direct vertical application, without any influence due to rotation of the joist and seat. The mechanism was observed only when the joist seat rested only on one outstanding leg. For the current testing, this would apply to the interior girder of each specimen but not the exterior girders. The joist seats rested across the entire top chords of the exterior girders and thus would not apply in this case. Also, the mechanism discussed by Galambos differed from that seen in the exterior girders, where an S-shaped buckle was produced as the joist seat rotated toward the interior girder and pulled upward on the outside outstanding leg of the joist-girder top chord. This buckle occurred because each joist seat was welded completely to a joist-girder top chord.

As a result of the problems encountered in the stub-girder tests, small stiffeners were added to the girder top chords beneath the load point locations for the haunched girder tests. The performances of the joist-girders in the haunched specimen were considerably better than the stub-girder specimen. No local buckling was observed in the top chords during the haunched girder testing, indicating that the stiffeners were more than adequate to prevent this local buckling.

CHAPTER V
SUMMARY AND CONCLUSIONS

5.1 Summary

The objective of this research was to analyze and compare methods of generating composite action in open-web joist-girders that have traditionally not been designed as composite entities within large floor systems. The results have also been examined to identify whether the model for composite joist design may be extended to joist-girders and accurately predict the performance of composite joist-girders.

Three configurations were theorized and designed by Nucor Research and Development. Three specimens were constructed at the Structures and Materials Research Laboratory at Virginia Polytechnic Institute and State University. The specimens were then tested to measure load capacity, deflections, strains, slips, etc. in order to observe how well the current method of composite design can be applied to systems where both the joists and joist-girders are designed to act compositely.

5.1.1 Flush Framed Girder Tests

The flush framed specimen was designed to utilize bolted connections to attach the joists to the joist-girders in such a way as to position all the top chords at the same elevation. This allowed the steel deck to rest directly on the joist-girders as well as the joists. Composite action could be generated in the joist-girders by welding shear studs directly to the top chords.

The specimen failed due to compression buckling of web members within joist-girder. The maximum experimental loads did not reach the predicted yield values calculated based on measured material properties for any of the joist-girders. Although the capacities were not modeled particularly well, the stiffnesses were predicted fairly well.

5.1.2 Stub-Girder Tests

The stub-girder specimen was designed to attach small hot-rolled sections, or "stubs," to the joist-girder top chords equal in height to the joist bearing seats. The steel deck was then placed on these stubs. The shear studs were then welded to the stubs to generate composite action in the stub-girders.

The specimen failed due to loss of shear connection and/or localized concrete crushing for each joist-girder. The top chord of EGR also buckled locally at the west joist bearing seat. The maximum experimental loads reached were significantly lower than the

predicted yield values calculated based on measured material properties. Although the capacities were not predicted closely, the stiffnesses were predicted quite accurately.

5.1.3 Haunched Girder Tests

The haunched girder specimen was designed to utilize built up haunches over the joist-girders. These haunches allowed the deck to be formed down to the joist-girder top chords so that shear studs could be attached directly to the girder top chords. The shear studs to be used were unusually long so that the heads of the studs reached into the compression zone of the concrete slab to generate composite action.

The specimen failed due to yielding of the bottom chords of the joist-girders. The maximum experimental loads reached or exceeded the yield values predicted based on measured material properties. The load capacities of the joist-girders proved to be more than adequate, especially for the interior joist-girder.

5.2 Conclusions

5.2.1 Flush Framed Girder Tests

- The "rigid support" design philosophy for the flush framed double angle vertical connection appears to work satisfactorily.
- Two inches of lateral concrete cover appears sufficient to develop the capacity of the shear studs on an exterior joist-girder when reinforcing bars are applied according to the test details.
- The installation of transverse reinforcement over the interior and exterior joist-girders can reduce the development of longitudinal shear planes over the joist-girders and thus reduce the potential for a decrease in moment capacity at these shear planes. However, a crack was observed over the interior joist-girder with only 30 k of applied load on IG. This crack did not appear to reduce the strength or stiffness of the composite joist-girder.
- The exterior joist-girders deflected laterally 0.05 in. without the bottom chord 9/16 in. diameter braces under a typical non-composite concrete, deck, and joist loading. These joist-girder rotations are not considered serviceability problems; therefore braces do not need to be installed for the exterior joist-girder bottom chord prior to placement of concrete in a typical building. These conclusions may be drawn for a composite joist-girder floor with 7 ft joists. It is unclear at this time whether or not the same conclusions may be drawn for a typical floor with 50 ft joists.
- The design model was fairly effective in predicting the joist-girder performances and conservative in computing the stiffnesses.

5.2.2 Stub-Girder Tests

- The significant variation in top chord cross section at the load points where the stubs were discontinued to accomodate the joist seats on the girder top chords produced a condition where three distinct, rigid regions formed along the joist-girder top chords. These regions were separated by hinge points that formed due to the concentrated joist reaction loads that were applied to the reduced cross-section.
- Deflection of the slab produced a significant rotation of the joist seats resting on the joist-girder top chords which in turn caused buckling in the horizontal legs of those joist-girder top chords. This condition would probably be magnified and become an even greater problem when using the longer, more typical joist spans encountered in actual structures.
- Transverse reinforcement over EGR, designed to provide the necessary minimum added strength to aid slab resistance to longitudinal shear, proved insufficient to carry the transverse tensile forces in the slab. The reinforcement was not able to adequately prevent cracking in the slab from this tension due to rotation of the slab parallel to the stud line away from the free edge.
- Noticeable yielding occurred in the bottom chords only in the panels directly below the joist seats at the girder third points. These zones picked up considerable tension as hinges formed in the top chords. Thus, unless some method were to be employed to stiffen the top chords at the third points, those locations in the bottom chords would become the critical areas for tension yielding, instead of at midspan.

5.2.3 Haunched Girder Tests

- The use of concrete haunches over open-web joist-girders appears to enhance the load carrying capacities of such girders. These haunches, in combination with significant reinforcement, provided considerably more strength than was anticipated. It would appear that this method is quite effective in providing composite strength. Alternatively, the design methodology could be considered overly conservative.
- Use of small stiffener plates to reinforce the top chords of the joist-girders at the load points appears to have worked very well. No local buckling or other phenomena were observed to have occurred at the load points of the joist-girders as a result of relative joist and slab rotation.
- Although the system demonstrated very good strength characteristics for the joist girders, consideration must be made of the fact that the haunch method requires a considerable amount of labor intensive preparation. Significant time and effort was required to fabricate the haunch forms that enclosed the joist seats. Labor input was also increased by the high amount of reinforcement as well as the number and size of shear studs that were installed.

5.3 Further Research

Based on the results of the testing reported here, and on observations made of the behavior and performance of the test specimens, several issues have been identified as possible focuses for future research efforts.

- Interaction of the joist seats on unstiffened joist-girder top chords during joist rotation, as in the stub-girder tests, should be looked at further. Non-composite frame testing could be performed to evaluate this mechanism in a more realistic configuration by allowing joists to be lengthened to a more realistic span length that would be encountered in the field.
- The results of the testing suggest that the current composite joist design method can only be applied in certain situations. This method should not be used for a stub-girder system. A new method needs to be developed in order to properly model the stub-girder system.
- Additional testing should be performed to better quantify the behavior of the flush framed and haunched setups. A number of parameters were varied for the construction of each setup, as well as during testing. These variations included the types of connections between the joists and joist-girders, not applying the loads from the joists to the joist-girder top chords in the flush framed setup, the addition of stabilizer blocks to the top chords of the haunched girders. These variations may have contributed to the variability in the results. Further study should be undertaken to look specifically at the mechanisms occurring within each type of joist-girder.
- Additional methods of generating composite action with joist-girders might also be theorized and explored.

REFERENCES

AISC. (1993). *Load and resistance factor design specification for structural steel buildings.* American Institute of Steel Construction, Chicago, IL.

Azmi, M. H. (1972). "Composite open-web trusses with metal cellular floor," Master of Engineering thesis, McMaster University, Hamilton, Ontario, Canada.

Bjorhovde, R., and Zimmerman, T. J. (1980). "Some aspects of stub-girder design." *Engineering Journal*, AISC, 17(3), 54-69.

Brattland, A., and Kennedy, D. J. L. (1992). "Flexural tests of two full-scale composite trusses." *Canadian Journal of Civil Engineering*, 9, 279-295.

Buckner, C. D., DeVille, D. J., and McKee, D. C. (1981). "Shear strength of slabs in stub-girders." *Journal of the Structural Division*, ASCE, 107(2), 273-280.

Chien, E. Y. L., and Ritchie, K. L. (1984). "Design and construction of composite floor systems." Canadian Institute of Steel Construction, Markham, Ontario, Canada.

Colaco, J. P. (1972). "A stub-girder system for high-rise buildings." *Engineering Journal*, AISC, 9(2), 89-95.

Curry, J. H. (1988). "Full-scale tests on two long-span composite open-web joists," MS thesis, University of Minnesota, MN.

Fahmy, E. H. A. (1974). "Inelastic analysis of composite open-web steel joists," MS thesis, McMaster University, Hamilton, Ontario, Canada.

Galambos, T. V. (1983). "Joists bearing on joist-girders: the performance and design checking of the chord-angle legs of the joist girders." *Structural Engineering Section, Report No. 1*, University of Minnesota, MN.

Gibbings, D. R., Easterling, W. S., and Murray, T. M. (1991). "Strength of composite long-span joists." *Report No. CE/VPI-ST 91/02*, Virginia Polytechnic Institute and State University, Blacksburg, VA.

Kigudde, M., Rambo-Roddenberry, M., Easterling, W. S., and Murray, T. M. (1998). "Flush framed composite joist girder tests." *Report No. CE/VPI-ST 96/11*, Virginia Polytechnic Institute and State University, Blacksburg, VA.

Lauer, D. F., Gibbings, D. R., Easterling, W. S., and Murray, T. M. (1996). "Evaluation of composite short span joists." *Report No. CE/VPI-ST 96/06*, Virginia Polytechnic Institute and State University, Blacksburg, VA.

"Limit states design of steel structures." (1989). *CAN/CSA-S16.1-M89*. Canadian Standards Association (CSA), Rexdale, Ontario, Canada.

Nguyen, S. T. (1992). "Elastic-plastic finite element modeling of long span composite joists with incomplete interaction," MS thesis,Virginia Polytechnic Institute and State University, Blacksburg, VA.

Oehlers, D. J. (1994). "Shear connection in haunched composite beams." *Journal of Structural Engineering*, ASCE, 120(7), 2227-2232.

"Proposed specification and commentary for composite joists and composite trusses." (1996). *Journal of Structural Engineering*, ASCE, 122(4), 350-358.

Rongoe, J. (1984). "A composite girder system for joist supported slabs." *Engineering Journal*, AISC, 21(3), 155-160.

Showalter, S. L., Rambo-Roddenberry, M., Easterling, W. S., and Murray, T. M. (1999a). "Composite stub joist girder tests." *Report No. CE/VPI-ST 97/02*, Virginia Polytechnic Institute and State University, Blacksburg, VA.

Showalter, S. L., Easterling, W. S., and Murray, T. M. (1999b). "Composite haunched joist girder tests." *Report No. CE/VPI-ST 97/03*, Virginia Polytechnic Institute and State University, Blacksburg, VA.

Tide, R. H. R., and Galambos, T. V. (1968). "Composite open-web steel joists." *Research Report No. 4*, Civil and Environmental Engineering Department Structural Division, Washington University, St. Louis, MO.

Wang, L. R., and Gotschall, J. A. (1980). "Computer-aided design of stub-girder system." *Engineering Journal*, AISC, 17(2), 25-32.